

AD-A057 338

GENERAL ELECTRIC CORPORATE RESEARCH AND DEVELOPMENT --ETC F/G 11/2
SILICON NITRIDE FOR AIRBORNE TURBINE APPLICATIONS.(U)

JUL 78 J A PALM, C D GRESKOVICH

N00019-77-C-0259

UNCLASSIFIED

SRD-78-076

NL

1 OF 2
AD
A057 338



END
DATE
FILMED
9-78
DDC

CONT.

AD A057338

LEVEL II



SILICON NITRIDE FOR AIRBORNE TURBINE APPLICATIONS

DDC FILE COPY

John A. Palm
Charles D. Greskovich
General Electric Company
Corporate Research and Development
P.O. Box 8
Schenectady, NY 12301

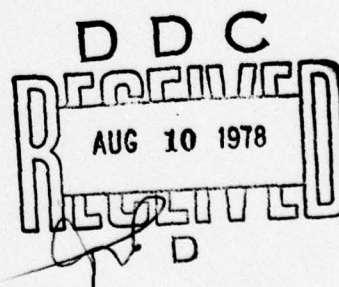
July 1978

Final Technical Report for Period 11 April 1977 - 11 April 1978

Approved for Public Release;
Distribution Unlimited

Prepared under Contract N00019-77-C-0259 for

NAVAL AIR SYSTEMS COMMAND
Department of the Navy
Washington, DC 20361



SRD-78-076

78 08 10 001

9

Final technical rept.
11 Apr 77-11 Apr 78

UNCLASSIFIED

SECURITY CLASSIFICATION OF THIS PAGE (When Data Entered)

REPORT DOCUMENTATION PAGE		READ INSTRUCTIONS BEFORE COMPLETING FORM
1. REPORT NUMBER	2. GOVT ACCESSION NO.	3. RECIPIENT'S CATALOG NUMBER
4. TITLE (and Subtitle)		5. TYPE OF REPORT & PERIOD COVERED
(6) SILICON NITRIDE FOR AIRBORNE TURBINE APPLICATIONS.		Technical Report - 4/11/77 - 4/11/78
7. AUTHOR(s)		8. PERFORMING ORG. REPORT NUMBER
(10) John A./Palm Charles D./Greskovich		(14) SRD-78-076
9. PERFORMING ORGANIZATION NAME AND ADDRESS		9. CONTRACT OR GRANT NUMBER(s)
General Electric Company Corporate Research and Development Schenectady, New York 12301		(15) N00019-77-C-0259 new
11. CONTROLLING OFFICE NAME AND ADDRESS		10. PROGRAM ELEMENT, PROJECT, TASK AREA & WORK UNIT NUMBERS
Naval Air Systems Command Department of the Navy Washington, D.C. 20361		(12) 47p.
14. MONITORING AGENCY NAME & ADDRESS (if different from Controlling Office)		12. REPORT DATE
		(11) Jul 1978
		13. NUMBER OF PAGES
		43
		15. SECURITY CLASS. (of this report)
		Unclassified
		15a. DECLASSIFICATION/DOWNGRADING SCHEDULE
16. DISTRIBUTION STATEMENT (of this Report)		
Approved for Public Release; Distribution Unlimited		
17. DISTRIBUTION STATEMENT (of the abstract entered in Block 20, if different from Report)		
18. SUPPLEMENTARY NOTES		
19. KEY WORDS (Continue on reverse side if necessary and identify by block number)		
Silicon Nitride, Synthesis and Powder Processing, Non-oxide Additives, Creep Resistance, Strength, Oxidation Resistance, Dynamic Fatigue, Fracture Toughness, Microstructure Control		
20. ABSTRACT (Continue on reverse side if necessary and identify by block number)		
<p>ALPHA</p> <p>Procedures are described for processing a commercially available α-Si_3N_4 powder which allow it to be hot-pressed to theoretical density when small additions of BeSiN_2 are added to the processed powder. Studies of the macro- and microstructural character of the hot pressed ceramic were conducted. The results of that study emphasized the need for thorough and homogeneous blending of the Si_3N_4 powder prepared and made ready for hot pressing. Investigations were conducted on the thermomechanical behavior of the fully dense hot pressed Si_3N_4 and measurements made at temperatures up to 1500°C of important thermomechanical properties. These properties included creep</p>		

DD FORM 1 JAN 73 1473 EDITION OF 1 NOV 65 IS OBSOLETE

UNCLASSIFIED

SECURITY CLASSIFICATION OF THIS PAGE (When Data Entered)

406 617

78

001

Jlu

UNCLASSIFIED

SECURITY CLASSIFICATION OF THIS PAGE(When Data Entered)

resistance, strength, dynamic fatigue and oxidation resistance. Comparison of these data were made with properties determined for NC-132, a commercial hot pressed Si_3N_4 ceramic.

ABSTRACT BY	
DTIC	White Section <input checked="" type="checkbox"/>
DDI	Diff Section <input type="checkbox"/>
UNANNOUNCED	<input type="checkbox"/>
JUSTIFICATION.....	
BY.....	
DISTRIBUTION/AVAILABILITY CODES	
Dist. AVAIL. REQ. BY SPECIAL	
A	

UNCLASSIFIED

SECURITY CLASSIFICATION OF THIS PAGE(When Data Entered)

SUMMARY OF RESULTS

1. The oxidation resistance at 1400°C in air of the hot-pressed Si_3N_4 containing 7% BeSiN_2 (nominal composition close to $\text{Si}_{2.9} \text{Be}_{0.1} \text{N}_{3.8} \text{O}_{0.2}$) was found to be exceptionally high in absolute terms as well as in comparison with the NC-132 reference material. In 210 hours for example, the weight gain per unit area for the material under study was found to be 0.74 g/m^2 as compared to 17.3 g/m^2 for NC-132.
2. Although the short time room temperature strength of the hot pressed Si_3N_4 containing 7% BeSiN_2 was found to be 345 MN/m^2 (50 kpsi) as compared to 862 MN/m^2 (125 kpsi) determined for NC-132, it was found to retain 88% of its room temperature strength when tested at short times at 1400°C. The NC-132 material was found to have lost 65% of its room temperature strength after short-time testing at 1400°C.
3. Measurements of time to failure at 3 different stressing rates indicated that at 1400°C the hot pressed Si_3N_4 containing 7% BeSiN_2 would have a strength after 10,000 hours of 241 MN/m^2 (35 kpsi) or 70% of its short time room temperature strength. In 10,000 hours at 1200°C NC-132 was found to have a strength of 269 MN/m^2 (39 kpsi), only 31% of its short time room temperature strength. A single point, strength determination of NC-132 at 1400°C suggested that under the best test conditions (using the same stressing rate employed for the 1200°C tests) it would have zero strength in about 1600 hours.
4. At 1400°C and under a stress of 69 MN/m^2 (10 kpsi) the BeSiN_2 doped material exhibited a creep resistance more than an order of magnitude greater than the NC-132 reference material.
5. The activation energy of creep for the hot pressed Si_3N_4 containing 7% BeSiN_2 was determined to be 176 Kcal/mole. The stress exponent n in the creep relationship, $\dot{\epsilon} = A\sigma^n \exp(-\Delta H/RT)$, was determined to be 1.1 for the hot pressed Si_3N_4 containing 7% BeSiN_2 indicating that under the test conditions employed the materials displayed Newtonian viscosity.
6. The creep resistance of hot pressed Si_3N_4 containing 7% BeSiN_2 was increased by ~3 times after annealing the hot pressed ceramic in N_2 for 24 hours at

1725°C. The corresponding grain growth that resulted due to the anneal was from about 0.5 μ to about 1.1 μ , indicating a bulk diffusion creep mechanism.

7. The room temperature fracture toughness (K_{1C}) of the hot pressed Si_3N_4 containing 7% $BeSiN_2$ was found to be about the same as the accepted value for sintered silicon carbide (SiC) and about one-half of the 7.3 $MN\ m^{-3/2}$ value determined for NC-132. Both determinations were made by the notched beam technique.
8. It has been shown that the oxygen content in the Si_3N_4 powder plays a dominant role in densification during hot pressing. It was found to affect the conditions of the hot pressing process as well as the final density of the product.
9. Intensive ball milling of Sylvania SN-502 Si_3N_4 powder, for 72 hours in benzene to increase its surface area from about 5 m^2/g to 13 m^2/g resulted in an increase in oxygen content from a measured value of 2.62% to 3.21%. Processing the milled powder to incorporate 7% $BeSiN_2$ added another 0.16% oxygen to the resulting powder. After hot pressing to full density, the resultant ceramic contained 3.1% oxygen.
10. A transient liquid phase which probably contains Si, Be, N and O forms and dissolves into the Si_3N_4 matrix. This phase is regarded as the critical step in the densification of Si_3N_4 and leads to a nearly single phase, hot-pressed product.

PREFACE

The research and development work described in this report was carried out within the Ceramics Branch of the Physical Chemistry Laboratory, at the General Electric Research and Development Center. It was conducted under Naval Air Systems Command Contract No. N00019-77-C-0259. Mr. I. Machlin of the Naval Air Systems Command was the Contract Monitor.

The program was directed toward the development and demonstration of compositions of Si_3N_4 which possess performance characteristics needed for airborne turbine applications. Specifically, this contract sought to evaluate the high temperature character and behavior of nearly theoretically dense Si_3N_4 ceramic consolidated by hot-pressing techniques and with non-oxide additives.

The authors acknowledge with their thanks the valuable consulting assistance in materials behavior and testing procedures graciously provided by Drs. S. Prochazka, R.J. Charles, and C.A. Johnson. The technical assistance of C.F. Bobik and C.R. O'Clair is also acknowledged with appreciation. Thanks are extended also to L. D'Amico for manuscript preparation.

TABLE OF CONTENTS

<u>Section</u>	<u>Page</u>
SUMMARY OF RESULTS	iii
PREFACE.	v
LIST OF ILLUSTRATIONS.	viii
LIST OF TABLES	ix
I. INTRODUCTION.	1
II. SYNTHESIS AND PROCESSING OF Si_3N_4 POWDERS	5
A. Si_3N_4 by Reaction Between Silane (SiH_4) and Ammonia (NH_3)	5
B. Si_3N_4 by Reaction Between Silicon Tetrachloride (SiCl_4) and NH_3	6
C. Processing of Commercial Si_3N_4 Powders.	7
1. Si_3N_4 Powder by H. Starck Co.	9
2. Si_3N_4 Powders by GTE-Sylvania	10
III. HOT PRESSED Si_3N_4 - PROCEDURES AND CHARACTERIZATION	17
A. Hot Pressing with BeSiN_2 Additive	17
B. Microstructural Characterization of Hot Pressed Si_3N_4	21
IV. EVALUATION OF THERMOMECHANICAL PROPERTIES OF HOT PRESSED Si_3N_4 CERAMIC FABRICATED FROM PROCESSED GTE SYLVANIA SN-502 Si_3N_4 POWDER CONTAINING 7% BeSiN_2	25
A. Oxidation Resistance.	25
B. Fracture Toughness.	28
C. Creep Resistance.	31
D. Strength.	34
V. CONCLUSIONS	41
REFERENCES	43
DISTRIBUTION LIST.	45

PRECEDING PAGE BLANK

LIST OF ILLUSTRATIONS

<u>Figure</u>		<u>Page</u>
1	Ammonium Chloride Separation and Decomposition of Silicon Diimide to Si_3N_4	8
2	Weight Loss and Specific Surface Area as a Function of Temperature for Si_3N_4 (SN-402) Powder Calcined in Vacuum (10^{-7} atm) for 30 minutes.	12
3	Relative Density as a Function of Applied Pressure for Two Processed Sylvania Powders of Same Particle Size but Different Oxygen Contents	19
4	Microstructure of Hot Pressed SN-502-1 Powder Containing 7 wt% BeSiN_2 Additive. $T=1780^\circ\text{C}$, $t=15$ min., N_2 . Reflected light - 1612X	20
5	TEM Photomicrograph of the Grain Structure in Hot Pressed Si_3N_4 Containing 7 wt% BeSiN_2 . In-House Si_3N_4 Powder Used During Fabrication - 68,000X.	22
6	TEM Photomicrograph of the Grain Structure in Hot Pressed Si_3N_4 Containing 7 wt% BeSiN_2 . In-House Si_3N_4 Powder Used During Fabrication - 150,000X	23
7	SEM Photomicrograph Showing Grain Size and Morphology of $\beta\text{-Si}_3\text{N}_4$, Hot Pressed Material - 7000X	23
8	SEM of the Typical Surface Character of Test Bars Used for Oxidation and Mechanical Testing - 200X	26
9	Oxidation Kinetics of Hot Pressed SN-502 Si_3N_4 Powder Containing 7% BeSiN_2	27
10	Oxidation Kinetics of Hot-Pressed NC-132 Si_3N_4	27
11	Configuration of Creep Test Specimen, Supports and Loading Fixtures.	31
12	Microstructure of As-Hot Pressed SN-502 Si_3N_4 Powder Containing 7% BeSiN_2 - 9,765X	33
13	Microstructure of Hot-Pressed SN-502 Si_3N_4 Powder Containing 7% BeSiN_2 After Annealing in N_2 at 1725°C for 25 h - 7,875X	34
14	$\log \dot{\epsilon}$ vs $1/T^\circ\text{K}$ Plot of Annealed and Unannealed Hot Pressed SN-502 Si_3N_4 Powder Containing 7% BeSiN_2 in Comparison with NC-132.	35
15	$\log \dot{\epsilon}$ vs $\log \sigma$ Plot of Hot-Pressed SN-502 Si_3N_4 Powder Containing 7% BeSiN_2 in Comparison with NC-132.	36
16	Stress vs Temperature for Hot-Pressed SN-502 Si_3N_4 Powder Containing 7% BeSiN_2 in Comparison with NC-132.	37
17	Time to Failure vs Relative Strength at Temperature	38

LIST OF TABLES

<u>Table</u>	<u>Page</u>
I Characterization of Starck Si_3N_4 Powder As-Received and Ball-Milled for 24 h in Benzene.	9
II Hot Pressing Results and Other Data on Processed Sylvania SN-502 Si_3N_4 Powder (Designation T-20609)	13
III Effect of Changes in Impurity Content as a Result of Leaching Milled Starck Si_3N_4 Powder on Relative Density of Hot Pressed Samples	14
IV Effect of Ceramic Processing on Oxygen Concentration of Sylvania SN-502 Si_3N_4	15
V Hot Pressed Billets for Machining into Thermomechanical Test Specimens	21
VI Weight Gain/Unit Area vs. Time in Air at 1405°C for NC-132 and Billet No. 3SN-(31). Billet Hot Pressed from Processed SN-502 Si_3N_4 Powder Containing 7% BeSiN_2	26
VII Room Temperature K_{IC} and γ_f for NC-132 Si_3N_4	29
VIII Room Temperature K_{IC} and γ_f for Processed SN-502 Si_3N_4 Powder Containing 7% BeSiN_2	30
IX Strain Rate Measurements ($\dot{\epsilon}, \text{h}^{-1}$) as a Function of Temperature.	32
X Strain Rate Measurements ($\dot{\epsilon}, \text{h}^{-1}$) as a Function of Stress	36
XI Short Time Modulus of Rupture at Room Temperature and at 1400°C	37
XII Time to Failure at 1400°C for Hot Pressed SN-502 Si_3N_4 Containing 7% BeSiN_2	38
XIII Time to Failure at 1200°C for NC-132 Si_3N_4	38

Section I

INTRODUCTION

Silicon nitride has been the subject of much effort by many workers to develop this material as a useful high temperature structural material. In this regard it has an important characteristic in its very low coefficient of thermal expansion, making it highly resistant to damage from thermal shock stresses. To be a useful structural material for high temperature applications, however, it must also meet a number of other requirements, such as oxidation resistance and resistance to deformation when stressed at elevated temperatures.

In the early considerations of SiC, prior to the development of new densification procedures, studies of the properties of single crystals gave strong evidence that pure polycrystalline SiC would be outstanding with respect to such requirements. To our knowledge, however, such prior evidence did not exist for silicon nitride. The characteristics of Si_3N_4 had been inferred from electronic and atomic structure. There was a need, therefore, for some experimental evidence of the properties of polycrystalline Si_3N_4 . In this regard oxidation and creep tests have been carried out by Greskovich and Rosolowski¹ on high quality CVD foils of Si_3N_4 . Experiments in three point bending at $\sim 1538^\circ\text{C}$ showed essentially no deflection after 198 hours at 69 MN/m^2 (10,000 psi). The material exhibited an upper creep limit of 10^{-7} h^{-1} outer fiber strain or creep rate at least five orders of magnitude less than seen in commercial silicon nitrides. Oxidation test by weight gain measurements showed a rate of $0.01 \text{ mg/cm h}^{1/2}$ at $\sim 1538^\circ\text{C}$, or about 10 times less than Si_3N_4 hot-pressed with 5% MgO and tested at $\sim 1100^\circ\text{C}$. Although the specific grain structure found in CVD Si_3N_4 makes generalizations of these results to a polycrystalline Si_3N_4 somewhat uncertain, it can be concluded that the intrinsic potential of Si_3N_4 as a high temperature structural material is indeed excellent.

Additional evidence further corroborates this conclusion. For instance, high-pressure hot pressing of various Si_3N_4 powders at 5500 MN/m^2 (800,000 psi) showed that the lowest temperature at which satisfactory bonding can be obtained (evaluated by microhardness indentation) is $\sim 1370^\circ\text{C}$; i.e., essentially the same as for SiC. This observation suggests that the atomic mobilities in SiC and Si_3N_4 are comparable, at least at this temperature, and that they are low enough to exclude yielding under any practical stress.

The self-diffusion studies by Wuench and Vasilos² gave an estimate of silicon diffusion in Si_3N_4 of $1.5 \times 10^{-13} \text{ cm}^2/\text{sec}$ at $\sim 1370^\circ\text{C}$ as compared to $2 \times 10^{-13} \text{ cm}^2/\text{sec}$ for the extrapolated diffusivity of silicon in SiC. Nitrogen diffusivities were not obtained in that work; however, recent results³ show that nitrogen diffusivity in Si_3N_4 is extremely low, near $10^{-18} \text{ cm}^2/\text{sec}$ at $\sim 1400^\circ\text{C}$. Other major characteristics of a material that determine its usefulness for high temperature applications are bulk strength and the dependence of the bulk strength on time and temperature. For the actual assessment of a material in a high-temperature load-bearing application, the relevant information sought by a designer is stress rupture performance; i.e., the interrelation of creep, oxidation and strength effects. The development of accurate stress rupture data on any material, however, is both difficult and exceedingly time consuming. As a consequence, extensive development of such data is rarely attempted for an emerging material that is continuously being subjected to modification. Procedures based on time-temperature parametric methods are used successfully for metals to extrapolate stress rupture behavior outside of the test range; unfortunately, a significant amount of test data at various stresses and temperatures must be available for reasonable accuracies of the extrapolations.

A theory of stress rupture in polycrystalline materials has been proposed recently⁴ whereby, given the activation energy for creep of the material, a single experimental stress rupture point and the exponent, n , of equation(1), the full range of stress rupture behavior of the material can be estimated, in principle:

$$\sigma^n \tau = \text{Constant} \quad (1)$$

σ = Applied Stress

τ = Time to Failure

The application of this theory to superalloys such as Nimonic 80A, pure metals, and lower temperature alloys such as 304 stainless steel gave results that were in good accord with extensive experimental information available on these materials. This theory has been utilized to estimate the short and long term stress rupture behavior of sintered, boron-doped SiC. By similar procedures, comparisons have been made with hot-pressed varieties of Si_3N_4 and SiC, with an early superalloy (Nimonic 80A), and with an advanced superalloy that is currently under development. Those comparisons indicated that at 1370°C the expected stress rupture characteristics of boron-doped sintered SiC exceed those of the other materials including the commercial forms of Si_3N_4 and SiC.

Such evaluations and estimates of the stress rupture behavior of sintered SiC are strongly dependent on the creep behavior of this material which, in turn, depends on intrinsic diffusional properties. The previous discussion pointed out that the intrinsic diffusional properties of Si_3N_4 are equivalent to those of SiC. Consequently, the stress rupture performance of an advanced form of pure phase Si_3N_4 is expected to be as good as that actually demonstrated for sintered SiC. Both materials, therefore, should show outstanding performance at temperatures in excess of 1370°C .

Although considerable progress has been made in the development of Si_3N_4 as a high temperature structural material, the various silicon nitride materials which have been evaluated, have been shown for a number of different reasons, to be unsuitable for long time operation at temperatures above about 1260°C .

The objective of this program was to obtain an early assessment of the potential of a new, sinterable Si_3N_4 composition by evaluating the high temperature character and behavior of nearly theoretically dense Si_3N_4 ceramic consolidated by hot-pressing techniques and with non-oxide additives. The approach employed to meet this objective was to (a) consolidate selected Si_3N_4 powder compositions in such a manner that oxide formation was avoided and essentially theoretical densities were achieved, through the use of non-oxide sintering aids such as Be_3N_2 and BeSiN_2 ; and (b) concurrent with the consolidation optimization studies, selected compositions were to be characterized and evaluated along with Norton NC-132 grade Si_3N_4 used as a reference material. Emphasis was to be placed on oxidation resistance and creep resistance at temperatures up to 1500°C . Other properties of interest, and preliminary values of which were to be obtained in this program, included strength, dynamic fatigue and fracture toughness.

Section II

SYNTHESIS AND PROCESSING OF Si_3N_4 POWDERS

During the initial stages of the program a variety of Si_3N_4 powders, from several sources were under active consideration and evaluation. From the results of a previous program (ARPA/AFML-F33615-76-C-5033) to study sintering processes in Si_3N_4 , and to develop densification methods for fabricating Si_3N_4 into useful components, it was concluded that success in the densification of Si_3N_4 by sintering, would require the availability of a high purity Si_3N_4 starting powder.

In order to provide a reproducible starting powder of high purity and large surface area, two synthesis routes were undertaken in addition to a program to evaluate certain commercial Si_3N_4 powders.

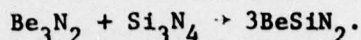
A. Si_3N_4 BY REACTION BETWEEN SILANE (SiH_4) AND AMMONIA (NH_3)

A detailed description of this powder making process has been previously documented⁵. This type of Si_3N_4 powder was prepared by reacting SiH_4 (electronic grade-Union Carbide Corp) and anhydrous NH_3 (dried with Ca_3N_2) at $\sim 650^\circ\text{C}$ using purified argon as a carrier gas. The gases were reacted in a fused silica reaction tube and the resulting product (Si_3N_4 smoke condensate) was accumulated by an electrostatic collector. The flow rates of the reactants and carrier gas employed in this synthesis route were $16\text{ cm}^3/\text{sec}$, $1.1\text{ cm}^3/\text{sec}$ and $8\text{ cm}^3/\text{sec}$ of SiH_4 , NH_3 and argon, respectively. Approximately 40 g of a light colored, yellowish-tan Si_3N_4 powder were produced by this method in ~ 6 h running time. This powder was found to be amorphous to X-rays. It had a powder density of 2.5 g/ml as determined by helium displacement and a specific surface area of $\sim 15\text{ m}^2/\text{g}$. It contained 3% oxygen impurity and $<1\%$ elemental Si. Exactly how the Si came to be formed was not determined. It seems likely however that it was formed either as a precipitate during the crystallization of the amorphous as-formed powder, or it was formed during the initial reaction between the SiH_4 and the NH_3 and was not subsequently nitrided to form the predominant Si_3N_4 product.

Greskovich, Prochazka, and Rosolowski⁵ summarized this Si_3N_4 synthesis route as being well understood and as a simple and practical process for preparation of laboratory quantities of Si_3N_4 . They further indicated that the process could be scaled up, but that there did not seem to be any fundamental

advantage over processes using considerably less expensive silicon halides in place of SiH_4 .

The 40 g of Si_3N_4 produced as described above from SiH_4 and NH_3 was prepared for hot-processing by mixing with it 2.8 g of BeSiN_2 , that had been previously synthesized according to the reaction:



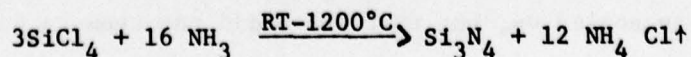
It had been determined that rather than making the Be addition in the form of Be_3N_2 to each batch of powder prepared for hot-pressing that the problems associated with the hygroscopicity of Be_3N_2 could be minimized by synthesizing the BeSiN_2 and using it as the Be additive compound. The BeSiN_2 is stable in the presence of water and was found to be the ideal Be addition compound to Si_3N_4 mixing of the 2.8 g of BeSiN_2 into the 40 g of Si_3N_4 powder was carried out by ball-milling the mix in a polyethylene jar mill containing ~180 ml of heptane and Si_3N_4 cubes as grinding media. The slurry was milled for 2 h and dried in air. The resulting powder was stored in a closed polyethylene jar and kept in a N_2 dry box until ready for hot pressing.

It was difficult to fabricate mechanically sound, hot pressed bodies with the as-formed amorphous Si_3N_4 powder synthesized from the $\text{SiH}_4\text{-NH}_3$ reaction. This difficulty was due, in large part, to the volume contraction occurring during hot pressing due to the amorphous-to-crystalline transformation at about 1450°C . Prior to hot pressing, this powder was calcined for ~15 min. in N_2 at 1450°C . The calcined powder was found to be a partially-crystallized $\alpha\text{-Si}_3\text{N}_4$ having a specific surface area of $\sim 9 \text{ m}^2/\text{g}$ and an oxygen content of about 2.8%.

These In-House powders were found to be easily hot pressed to essentially theoretical densities. However, a commercial powder was subsequently found, after processing, to yield equally good hot-pressed material. Thus the preparation of In-House powder used for fabricating thermochemical test specimens was de-emphasized.

B. Si_3N_4 BY REACTION BETWEEN SILICON TETRACHLORIDE (SiCl_4) AND NH_3

Laboratory quantities of Si_3N_4 were also synthesized by the procedures reported by Mazdiasni and Cooke⁶ through an overall chemical reaction that could be written as:



The intermediate reaction chemistry was known to be quite complex and probably not completely understood because of the formation, polymerization reactions and decomposition of silicon diimide and the complications associated with the formation and management of the NH_4Cl by-product.

In practice SiCl_4 and NH_3 were reacted in hexane cooled with dry ice. The reaction products $\text{Si}(\text{NH}_2)_4$ and NH_4Cl still contained in hexane were transferred to the short inner mullite crucible shown in Figure 1 which was then assembled in the larger mullite reactor tube. The reactor assembly was then completed with its Pyrex Cap, thermocouple and gas inlet tube. After purging the system thoroughly with a 6:1 volume ratio of argon: H_2 , the outer reactor tube was carefully heated to first distill off the hexane and with continued heating permit the various reactions to take place which lead to the final product. A terminal temperature of about 1300°C was found necessary to form the amorphous Si_3N_4 . By continuing the heating of that product to $\sim 1500^\circ\text{C}$, the calcination and conversion of the amorphous material to the crystalline product was carried out without exposing the amorphous and highly reactive product to the air atmosphere. X-ray diffraction analyses confirmed this product to be $\alpha\text{-Si}_3\text{N}_4$. Surface areas were determined to be as high as $100 \text{ m}^2/\text{g}$ on the amorphous Si_3N_4 powders produced in this manner. Calcining the amorphous powders as described above resulted in reduction of surface areas to measured values of $25 \text{ m}^2/\text{g}$. Further reductions in surface areas could be expected with longer calcining times. Preliminary densification experiments demonstrated that the Si_3N_4 powders produced by the above synthesis route could be sintered to 93% of theoretical using 1% additions of Be as Be_3N_2 . Although we were confident that scale-up of the process would successfully produce larger quantities of Si_3N_4 needed for the fabrication of thermomechanical test specimens, continued development of this operation was suspended in favor of working with a commercially available powder synthesized from the same reactants.

C. PROCESSING OF COMMERCIAL Si_3N_4 POWDERS

While the investigations into the synthesis of Si_3N_4 powders were proceeding, an evaluation of two commercial sources of Si_3N_4 powders was undertaken. One of these was a product from the H. Starck Co. This powder was made by the nitridation of silicon process. Two powders manufactured by GTE-Sylvania and designated as SN-402 and SN-502 were evaluated. These powders were derived from a $\text{SiCl}_4\text{-NH}_3$ type reaction.

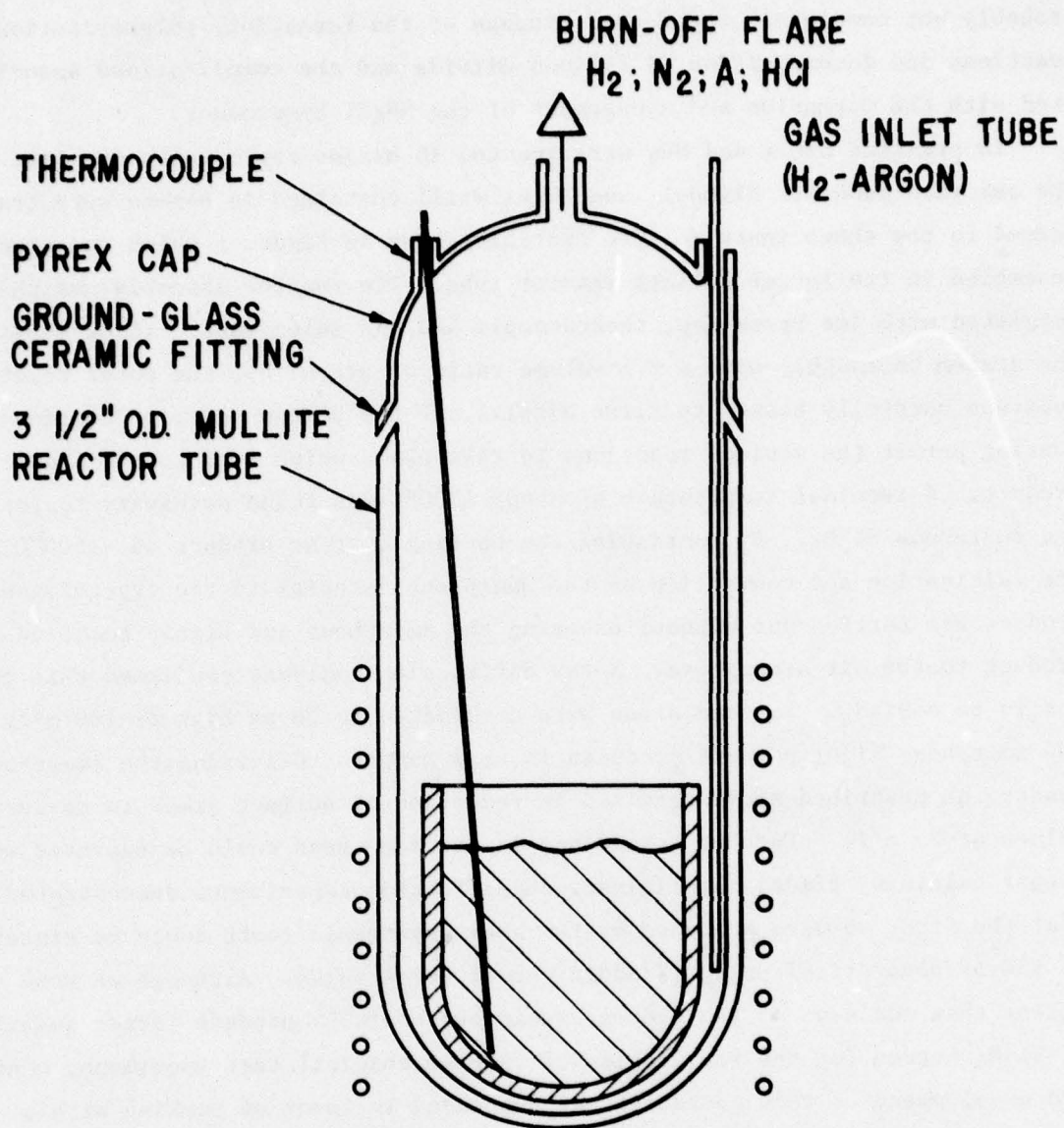


Figure 1. Ammonium Chloride Separation and Decomposition of Silicon Diimide to Si₃N₄

This section describes the evaluation work conducted on these three commercial Si_3N_4 powders manufactured by two different processes.

1. Si_3N_4 Powder by H. Starck Co. In order to reduce the particle size of the as-received powder to a level in the 8-15 m^2/g range, it was ball-milled using steel balls for 24 h in benzene. After removal of the benzene the milled powder was leached with a 5% HCl solution to remove iron that had been milled into the powder. Thorough water washing was then employed to remove all traces of soluble Fe and Cl ions. Impurity levels in the as-received and ball milled powders are shown in Table I. This Table also compares surface area and powder densities of the as-received and milled powders.

Table I		
CHARACTERIZATION OF STARCK Si_3N_4 POWDER AS-RECEIVED AND BALL-MILLED FOR 24 H IN BENZENE		
Chemical Element	As-Received (Wt.%)	Milled and Leached (Wt.%)
Al	0.18	0.21
Fe	0.07	0.07
Ca	0.12	0.10
Mg	0.03	0.03
C	0.6	0.6
Si(excess)	<1.0	<1.0
O	1.1	1.5
Surface Area (m^2/g)	7.8	13.9
Powder Density (g/cc)	3.15	3.15

The as-received powder contained metallic impurities typical of most commercially-available Si_3N_4 powders produced by nitridation of Si. On the other hand, the oxygen content of the as-received powder was found to be quite low and probably related to the presence of a considerable amount of carbon (0.6 wt%) which, perhaps, permitted the attainment of low oxygen activities during nitridation. Milling permitted two major changes to occur. The specific surface area and oxygen content both increased to 13.9 m^2/g and 1.5 wt%, respectively. They fall in the desired range of values (8-15 m^2/g and 1-3 wt%) which permit high densification rates during hot pressing when Be_3N_2 or BeSiN_2 was used as a densification aid.

Further characterization of this powder involved determination of whether the carbon content was in the free or combined state. Because of the low carbon content on a percentage basis, it was decided to thermally decompose 0.5 g of Starck Si_3N_4 powder at 1500°C under vacuum for 2 h in the hope that a high carbon containing residue might remain. There was about 80% weight loss during this heat treatment. The residue material was collected and examined by X-ray diffraction. A distinct peak of $\beta\text{-SiC}$ was observed. Therefore, it was concluded that there was about 2 wt% $\beta\text{-SiC}$ in the "as-received" Starck powder, assuming all of the 0.6 wt% C was combined with Si to form $\beta\text{-SiC}$.

Because of the concern about the probable deleterious effect of Ca on the creep resistance of Si_3N_4 ceramic, an attempt was made to determine if the 0.1% Ca content found in the as-received Starck powder could be lowered by chemical leaching to a level closer to 100 ppm. It was determined that after the initial leaching of the ball milled Starck Si_3N_4 with HCl primarily to remove Fe milled into the powder there was a lowering of the Ca content to between 0.06% and 0.07%. This level could not be lowered any further by additional room temperature and hot (80°C) leachings with 7% and 20% NaOH solutions, respectively.

Although it was found that the Starck Si_3N_4 powder could be hot-pressed to essentially theoretical density with 1% Be additions in the form of BeSiN_2 , it was our opinion that better thermomechanical properties would be obtained from a Si_3N_4 ceramic having considerably less Ca content than we were able to obtain by the chemical processing of the Starck powder. Consequently, no further large scale efforts were expended with this material.

2. Si_3N_4 Powders by GTE-Sylvania. Another high purity Si_3N_4 powder that was investigated was an amorphous form designated as SN-402 by GTE-Sylvania.

The as-received powder had a metallic purity of ~99.99 wt% with the major impurity being ~0.01 wt% Mo. The oxygen content determined by neutron activation analysis was ~3 wt%. Supplier specifications indicates the powder to contain <1 wt% Cl and exhibit a specific surface area between 10 and 60 m^2/g . Our lot of Si_3N_4 powder was found to have a specific surface area of 30 m^2/g .

Optimization of this powder to subsequent use was achieved by calcination in vacuum at various temperatures and measuring specific surface area and weight loss. This calcination treatment served the purpose of (1) removing some chlorine which was believed to retard densification during hot pressing, (2) crystallize the amorphous powder into $\alpha\text{-Si}_3\text{N}_4$ and (3) reduce the specific surface

area from 30 to about $10 \text{ m}^2/\text{g}$ so that reasonably high powder compaction could take place in the die before hot pressing. The results of the calcination treatments are shown in Figure 2. A rapid reduction in specific surface area and a marked rise in weight loss occurred between 1200 and 1400°C. Powder calcined at 1200°C for 0.5 h in vacuum was essentially amorphous and white. Powder calcined at 1300 and 1400°C was light and dark tan, respectively, and in both cases composed of essentially $\alpha\text{-Si}_3\text{N}_4$ as determined by X-ray diffraction analysis. Based on this information and past experience with producing sinterable and densifying Si_3N_4 powders for hot pressing, a temperature of 1300-1325°C was selected as the optimum calcination temperature for this Sylvania SN-402 powder.

It should be pointed out here that when this lot of Sylvania SN-402 powder, calcined at 1325°C in vacuum, was milled with 2% Be_3N_2 or 7 wt% BeSiN_2 (~1% Be) as a densification aid and subsequently hot pressed at 70 MPa (10,000 psi) for 15 min. at 1800°C, relative densities greater than 85% were not achieved. Curiously, however, relative densities ~96% of theoretical were obtained with a small batch of SN-402 powder purchased more than 2 years prior to this most recent purchase and similarly processed. These results tended to suggest that for our purposes Sylvania's SN-402 powder would require special processing (milling and leaching) to produce a final powder which would give rise to full densification during hot pressing.

The work on SN-402 was followed by some additional work with another Sylvania Si_3N_4 powder designated as Sylvania SN502, a crystalline form of that compound, and predominantly of the α modification. About 2.3 kg of the SN502 Si_3N_4 powder was purchased and designated as T-20609. Two ball mills were charged with 200g each of this powder and ball-milled for 72 hours in benzene. The ball-milled powder from each mill was HCl-leached to remove iron contamination from the milling operation. The surface areas of the 2 different millings were $11.4 \text{ m}^2/\text{g}$ and $10.4 \text{ m}^2/\text{g}$ showing good reproducibility in milling results. One of the 2 milled lots of SN502 was checked for hot pressed densification using 7 w/o BeSiN_2 . A small 5 mm pill densified almost completely (98.5% theoretical). This result was encouraging because the synthesis route for making the SN502 indicated that Ca impurity should be extremely low, perhaps <6 ppm. About 100g of the milled SN502 was processed to allow a 5 cm diameter billet to be hot pressed.

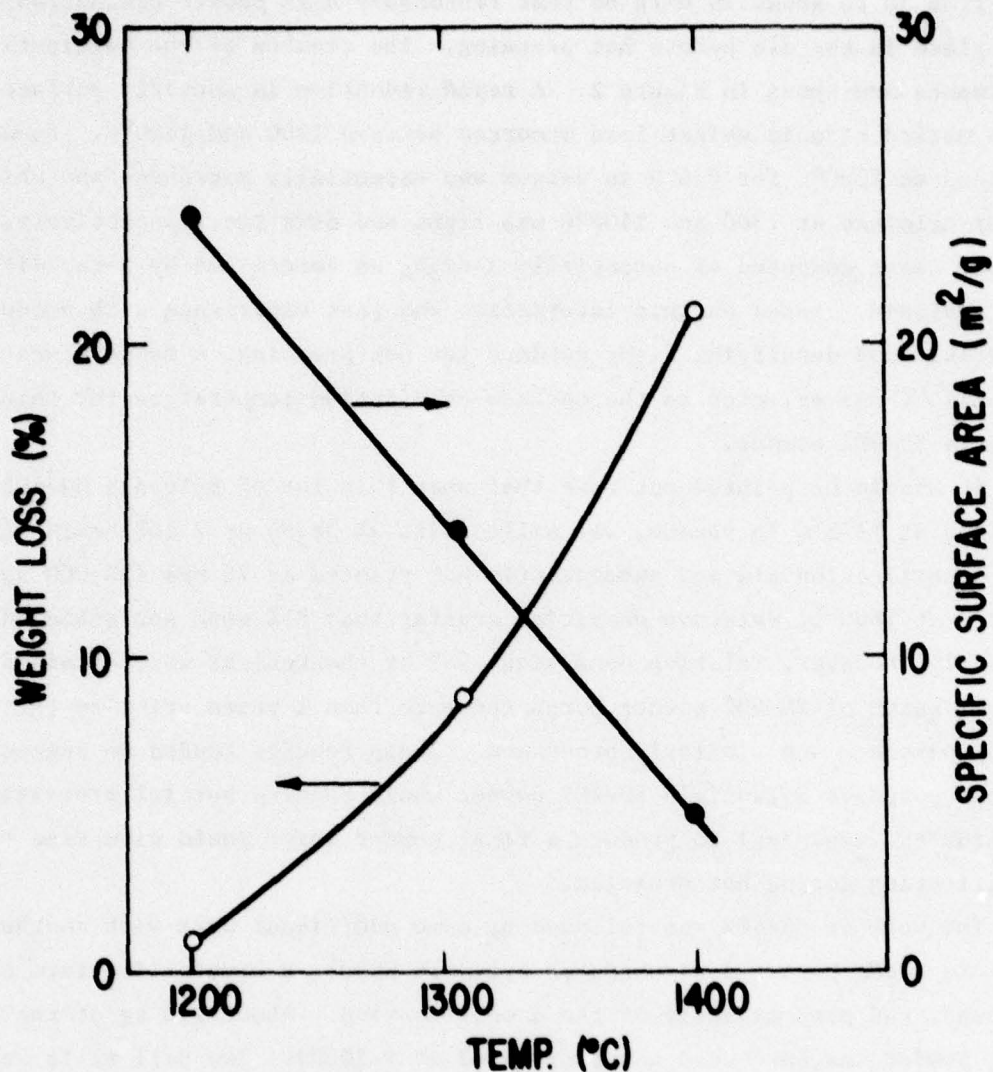


Figure 2. Weight Loss and Specific Surface Area as a Function of Temperature for Si_3N_4 (SN-402) Powder Calcined in Vacuum (10^{-7} atm) for 30 Minutes

To further check on the reproducibility of the chemical processing on the SN502 a larger mill size was employed in the next experiment. A 1200g charge of the same lot (T-20609) of SN502 was milled in a single ball mill for 72 hours in benzene. The product was dried and a 50g portion of it was leached with HCl and washed free of Fe and Cl. Its surface area was measured and found to be $13.3 \text{ m}^2/\text{g}$. A small 5 mm diameter pill of this material with 7 w/o of BeSiN_2 was hot pressed to a density 97.5% of theoretical. These results

from experiments utilizing the Sylvania SN502 Si_3N_4 powder indicated that satisfactory processing and hot pressing reproducibility could be easily achieved with this material. Consequently the bulk of the milled 1.2 kg of powder was HCl-leached and washed. This powder was then set aside for use in hot pressing sufficient 5 cm dia. billets to provide the necessary test pieces for measuring the mechanical properties and oxidation resistance of this material. The data obtained from the experiments with Sylvania's SN502 Si_3N_4 powder are shown in Table II. Because it was found that this high purity, (essentially Ca-free) commercially available Si_3N_4 powder could be reproducibly densified to nearly theoretical density, it was decided that this would be the Si_3N_4 powder from which billets would be hot-pressed for the fabrication of thermomechanical test specimens.

Table II
HOT PRESSING RESULTS AND OTHER DATA ON PROCESSED SYLVANIA SN-502
 Si_3N_4 POWDER (DESIGNATION T-20609)

<u>Powder Identification</u>	<u>Surface Area(m^2/g)</u>	<u>Hot Pressed Density with 7% BeSiN₂(% Theoretical)</u>
200 g as-received milled and HCl-leached (SN-502-I)	11.4	98.5
200 g as-received milled and HCl-leached (SN-502-II)	10.4	97.5
1200 g as-received milled and HCl-leached (SN-502-23)	13.3	99

Additional powder characterization studies conducted on the GTE-Sylvania SN-502 powder showed that the 72 h ball-milling of the powder to reduce its particle size also increased its bulk density from a value of 0.1266 g/cm^3 to 0.5883 g/cm^3 , a 4.5 times reduction in its powder volume per unit weight. Analytical results showed that this processed powder, after being mixed with 7% BeSiN₂ and ready for hot-pressing contained 3.24% oxygen and ~0.008% Fe. No Ca was detected indicating that it contained less than the limit of detection technique (.03%).

In one investigation on the effect of changes in impurity content as a result of leaching milled Starck powder on the relative density of hot pressed samples it appeared that the oxygen content in the powder might have a significant effect on the density that could be achieved in the hot-pressed billet. Those results on the Starck powder are shown in Table III.

Powder Identification	Surface Area (m^2/g)	Impurities			Relative Density with 7% BeSiN ₂ Additive
		%O	%Ca	%Fe	
Milled and HCl-Leached Starck Si_3N_4 Powder	13.5	1.47	.06	.01	79.4
Milled and HCl-Leached Plus NaOH-Leached Starck Si_3N_4 Powder	14.2	1.26	.06	.003	70.0
Milled and HCl-Leached Plus "Hot" NaOH-Leached Starck Si_3N_4 Powder	----	0.93	.07	----	71.0

*Applied pressure of 69 MN/m^2 (10,000 psi) for 15 min. at 1780°C .

Since it appeared that the oxygen content of the Si_3N_4 powder may affect (and even control) the density of the hot pressed billet, it was decided to determine quantitatively the effect of ceramic processing on the oxygen concentration in the resulting SN-502 Si_3N_4 powder. The oxygen content was measured by neutron activation analysis with a standard deviation of about ± 0.01 wt% at oxygen levels of 1-3 wt%. The results are shown in Table IV. The as-received, Sylvania SN502 Si_3N_4 powder had a specific surface area of $\sim 5 \text{ m}^2/\text{g}$ and an oxygen content of 2.62 wt%. By increasing the specific surface area of this powder by ball-milling to $\sim 13 \text{ m}^2/\text{g}$, there was a corresponding increase in the oxygen content to 3.21 wt%. If the oxygen content was combined in the form of SiO_2 , then 3.21 wt% O is equivalent to about 6 wt% SiO_2 . Calculations show that a $\sim 13 \text{ m}^2/\text{g}$ Si_3N_4 powder should have an oxygen content of ~ 1 wt% due to a monomolecular layer of SiO_2 on the Si_3N_4 particle surfaces. The much higher oxygen contents measured was probably associated with the presence of free SiO_2 particles, unassociated with Si_3N_4 surfaces, and/or $\text{Si}_2\text{N}_2\text{O}$ particles

Table IV
EFFECT OF CERAMIC PROCESSING ON OXYGEN
CONCENTRATION OF SYLVANIA SN-502 Si_3N_4

<u>Powder Condition</u>	<u>Oxygen Content*(wt%)</u>
SN502, as-received ($\sim 5 \text{ m}^2/\text{g}$)	2.62
Milled SN502 (72h) and HCl-leached ($13 \text{ m}^2/\text{g}$)	3.21
Mixed (1h) composition of milled SN502 powder and 7 wt% BeSiN_2	3.37
Hot pressed sample of mixed composition (fully dense)	3.10

*Measured by neutron activation analysis.

in these Si_3N_4 powders. The mixing step, where 7 wt% BeSiN_2 was added, caused the oxygen content of the powder mixture to increase to 3.37 wt%. The 0.16 wt% oxygen acquired was probably due to the presence of ~ 2 wt% oxygen in the BeSiN_2 additive. Finally, the oxygen content of the dense, hot-pressed Si_3N_4 sample was found to be slightly lower, 3.1 wt%, than the mixed composition. The decrease was probably associated with oxygen loss via SiO evolution during the hot pressing stage which took place in a nitrogen atmosphere ($\text{PO}_2 < 10^{-5} \text{ atm}$) at 1780°C . This hot pressed sample was found to be essentially single phase, $\beta\text{-Si}_3\text{N}_4$ solid solution by X-ray diffraction and optical microscopy. Thus an optimum amount of oxygen and BeSiN_2 were present in the batch composition. These results confirmed earlier, non-systematic findings which showed that high density-single phase $\beta\text{-Si}_3\text{N}_4$ can be produced from Si_3N_4 powders having 2.5 to 3.5 wt% O, specific surface areas between about 10 and $15 \text{ m}^2/\text{g}$ and $\sim 5\text{-}7$ wt% BeSiN_2 as a densification aid.

Section III

HOT PRESSED Si_3N_4 - PROCEDURES AND CHARACTERIZATION

A. HOT PRESSING WITH BeSiN_2 ADDITIVE

As discussed in earlier sections the SN-502 Si_3N_4 powder as-received from GTE-Sylvania was processed by ball-milling in order to increase its surface area from $\sim 5 \text{ m}^2/\text{g}$ to $\sim 13 \text{ m}^2/\text{g}$. After leaching the milled product with HCl to remove Fe contamination from the milling operation the washed and dried powder was doped with 7% BeSiN_2 (1% Be). BeSiN_2 was found to be excellent densification aid for pure or impure Si_3N_4 powders. It has allowed hot pressed densities close to 100% of theoretical to be realized. Additionally, at high temperatures it will dissolve into the $\beta\text{-Si}_3\text{N}_4$ lattice leading to a single phase material as determined by X-ray analysis. As will be shown in the following sections the BeSiN_2 also imparts outstanding oxidation resistance quality to the Si_3N_4 ceramic. When combined with the processed SN-502 Si_3N_4 powder as a densification aid, the resulting hot-pressed material was found to exhibit superior mechanical properties behavior at high temperatures.

The preparation of a batch of powder was carried out in the following manner.

Processed SN-502 Si_3N_4 powder, (52.0)g and 3.64 g of BeSiN_2 powder were mixed in a Nalgene bottle containing 170 ml heptane (99%) and 5 drops of oleic acid. Two hundred, Si_3N_4 ceramic cubes were included as a mixing and milling aid. The entire mix was mixed on a paint shaker for 3 hours. The heptane was evaporated from the bottle and the dry powder and Si_3N_4 cubes were dry mixed on the paint shaker for another 1/2 h. After separating the cubes from the powder it was ready to be hot pressed.

Generally before hot pressing a 5 cm dia. billet, a small pill of the powder was hot pressed to check the densification quality. These small hot press quality checks always showed pill densities of 99.8% of theoretical were achieved.

Conventional hot pressing procedures were employed using two Poco^R graphite dies, 1 and 5 cm in diameter. The smaller die as just described was used more frequently because of faster "turn-around" time. Approximately 0.5 to 1 g samples were hot pressed in the small die whereas 50 to 100 g of powder was

hot pressed in the large die. To prevent reactivity of the Si_3N_4 powder with graphite during hot pressing, the wall of the die and the plunger faces were coated with a BN or SiC slurry before powder loading.

The temperature-pressure cycle for a typical hot pressing run consisted of (1) evacuating to less than 1 torr and filling with N_2 gas; repeat, (2) applying a pressure of 3.5 MPa at room temperature and the final desired pressure at 1100-1200°C. The time to reach 1750°C, for example, was 15 to 20 min. After a soak time of 15-20 min in nitrogen, the power to the induction coils was turned-off and the applied pressure either removed or reduced during cooling. The BN or SiC coating was removed from the resulting hot pressed sample before characterization.

It was our experience that different commercial lots of Si_3N_4 powder exhibited different hot pressing behavior even though the ceramic processing and concentration of BeSiN_2 additive were identical. In particular the applied pressure required to achieve full density appeared to depend on the chemical nature of the starting Si_3N_4 powder. This is illustrated in Figure 3 for two processed powders of the same "nominal" composition and nearly the same average particle size. The relative density of SN502-1 processed powder rose sharply with increasing applied pressure between 14MN/m² (2,000 psi) and 25MN/m² (3,700 psi) such that nearly theoretical density was achieved at about 25MN/m² at 1780°C for 15 min in N_2 . Higher applied pressures resulted in little change in final density of the Si_3N_4 samples. In contrast, it was very difficult to hot press fully dense Si_3N_4 billets made from SN502-23 powder composition unless the maximum applied pressure of $\approx 70\text{MN/m}^2$ (10,000 psi) was employed. These results combined with the general observation that denser samples usually had a lower specific surface area in the open porosity stage of densification suggested that the difference in shapes and magnitudes of the density vs. pressure curves were not due to widely different driving forces for densification but must be related to differences in mobility of the diffusing species. It was speculated that both the SN502-1 and SN502-23 powder compositions densified via a transient liquid phase mechanism, and in the SN502-1 material either a greater volume of liquid phase was present during hot pressing or this liquid remained undissolved in the $\beta\text{-Si}_3\text{N}_4$ lattice until higher temperatures were reached. This further implied, that the oxygen content of the SN502-1 processed powder should be higher than that of the SN502-23 processed powder. This was indeed found to be true by measurement of oxygen content in both powders, the results of which are designated in Figure 3.

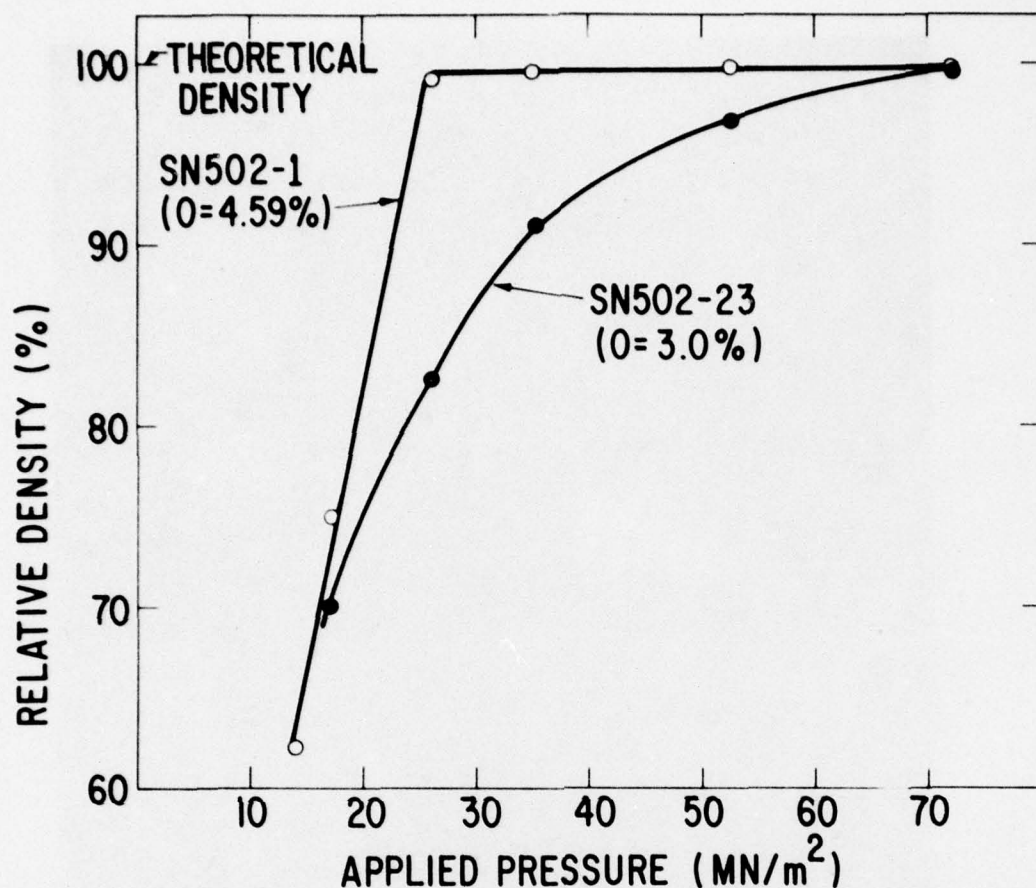


Figure 3. Relative Density as a Function of Applied Pressure for Two Processed Sylvania Powders of Same Particle Size but Different Oxygen Contents. Samples were hot pressed at 1780°C for 15 min in N_2 , and contain 7 wt% $BeSiN_2$ as a densification aid.

Figure 4 shows a high magnification photomicrograph of the microstructure of hot pressed SN502-1 Si_3N_4 powder containing 7 wt% $BeSiN_2$ additive. The light grey matrix material is β - Si_3N_4 solid solution, the bright (white) particles are silicon and the dark grey phase is Si_2N_2O . X-ray diffraction helped elucidate the identification of these phases. In contrast, hot-pressed samples derived from SN502-23 powder contained virtually no Si_2N_2O phase. A look at these results in light of the recently published phase diagram⁽⁷⁾ for the Si_3N_4 - Be_3N_2 - BeO - SiO_2 system indicated that if the high SiO_2 content of ≈ 4.6 wt% in the mixed, processed powder (SN502-1) cannot be consumed by reaction with the $BeSiN_2$ additive to completely dissolve into the β - Si_3N_4 lattice, then residual Si_2N_2O phase will be present in equilibrium with β - Si_3N_4 solid solution. On the other hand, it is possible that unknown impurities in the SN502-1 powder stabilize the Si_2N_2O phase to higher temperatures and is necessary for the achievement of full density during hot pressing.

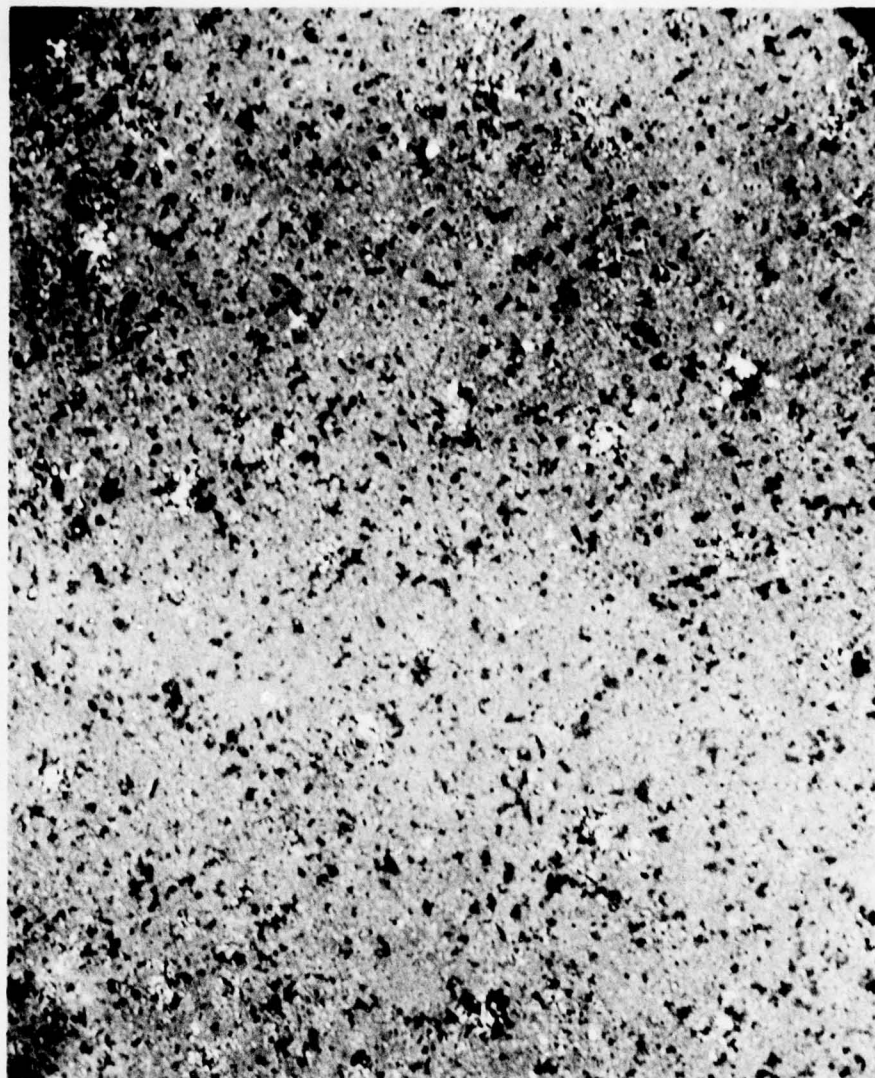


Figure 4. Microstructure of Hot Pressed SN-502-1 Powder Containing 7 wt% BeSiN_2 Additive. $T=1780^\circ\text{C}$, $t=15$ min., N_2 . Reflected light - 1612X.

Four hot-pressed billets about 5 cm (2.0 in) in diameter by about 1.3 cm (0.5 in) in thickness were made essentially by conventional hot pressing procedures described above. Data on the fabrication of these three billets are shown in Table V. Billets designated as ISN-(25) and 2SN-(26) were set aside for fabrication into bend test bars. Billet number 3SN-(31) was reserved for fabrication into creep test bars and billet number 4SN-(49) was used for fabrication of notched beam test specimens for determination of fracture toughness (K_{1C}).

TABLE V				
HOT-PRESSED BILLETS FOR MACHINING INTO THERMOMECHANICAL TEST SPECIMENS				
Billet No.	Original Si_3N_4 Powder Source	Processing on As-Received Powder and Processed Powder Designation	Processed Powder Surface Area (m^2/g)	Hot-Pressed Billet Density with 7% BeSiN_2 (g/cm^3)
1SN-(25)	Sylvania SN-502 (Lot Designation T-20609)	Wet Milling in benzene (72 h) HCl Leaching and Washing until Fe and Cl Free (SN502-1)	11.4	3.13
2SN-(26)	Sylvania SN-502 (Lot Designation T-20609)	Wet Milling in benzene (72 h) HCl Leaching and Washing until Fe and Cl Free (SN502-1)	11.4	3.12
3SN-(31)	Sylvania SN-502 (Lot Designation T-60596)	Wet Milling in benzene (72 h) HCl Leaching and Washing until Fe and Cl Free (SN502-23A)	13.3	3.15
4SN-(49)	Sylvania SN-502	Wet Milling in benzene (72 h) HCl Leaching and Washing until Fe and Cl Free (SN502-23A)	13.3	3.17

B. MICROSTRUCTURAL CHARACTERIZATION OF HOT PRESSED Si_3N_4

The microstructure of hot pressed Si_3N_4 prepared with In-House silane derived Si_3N_4 and 7 wt.% BeSiN_2 used as a densification aid has been examined. X-ray diffraction patterns of the hot pressed material showed the presence of only the β -form of Si_3N_4 . Observation of polished specimens in reflected light revealed that a small amount of ($<1\%$) of Si particles $<5\mu$ in size existed in the microstructure. This information combined with the fact that the a and c lattice parameters decrease for BeSiN_2 -doped Si_3N_4 compared to pure Si_3N_4 indicate that the composition of the β - Si_3N_4 solid solution is close to $\text{Si}_{2.9}\text{Be}_{0.1}\text{N}_{3.8}\text{O}_{0.2}$.

The microstructure was then examined at higher magnification than that possible by optical microscopy by employing transmission electron microscopy. Transmission electron microscopy was used to elucidate if a boundary phase could be detected between β - Si_3N_4 grains. Specimen preparation involved: (1) grinding a thin slice of the sample with 600 grit SiC to a thickness of about 50 microns, (2) micromilling from both sides of the specimen with 6 kV Ar ions at an angle of 21° until a small hole formed in the center of the specimen and (3) examining the specimen in bright field transmission in a multitilt, Siemens Elmiskop 101 microscope at 125 kV. Approximately 100 grain boundaries were examined for a grain boundary phase.

Transmission electron micrographs of an ion-thinned specimen shown in Figures 5 and 6 illustrate the microstructure of the material. Figure 5 indicates the average size of the β -grains is about $0.8\ \mu$. Note that the β - Si_3N_4 grains are equiaxed rather than elongated as is usually found in commercial forms of hot pressed Si_3N_4 . This observation is further confirmed by the SEM photomicrograph of a polished and chemically-etched section of hot pressed material of the same composition shown in Figure 7. The grain structure is composed of equiaxed β - Si_3N_4 grains which approximate the classical "soap bubble" structure for a single phase material. Finally, no evidence of an intergranular glassy phase was detected by conventional transmission electron microscopy. Over 100 grain boundaries were viewed in the electron microscopy with tilting capability but no grain boundary phase was observed. However, preliminary results of lattice fringe imaging using TEM show an intergranular phase $<10\text{\AA}$ thick on some grain boundaries.

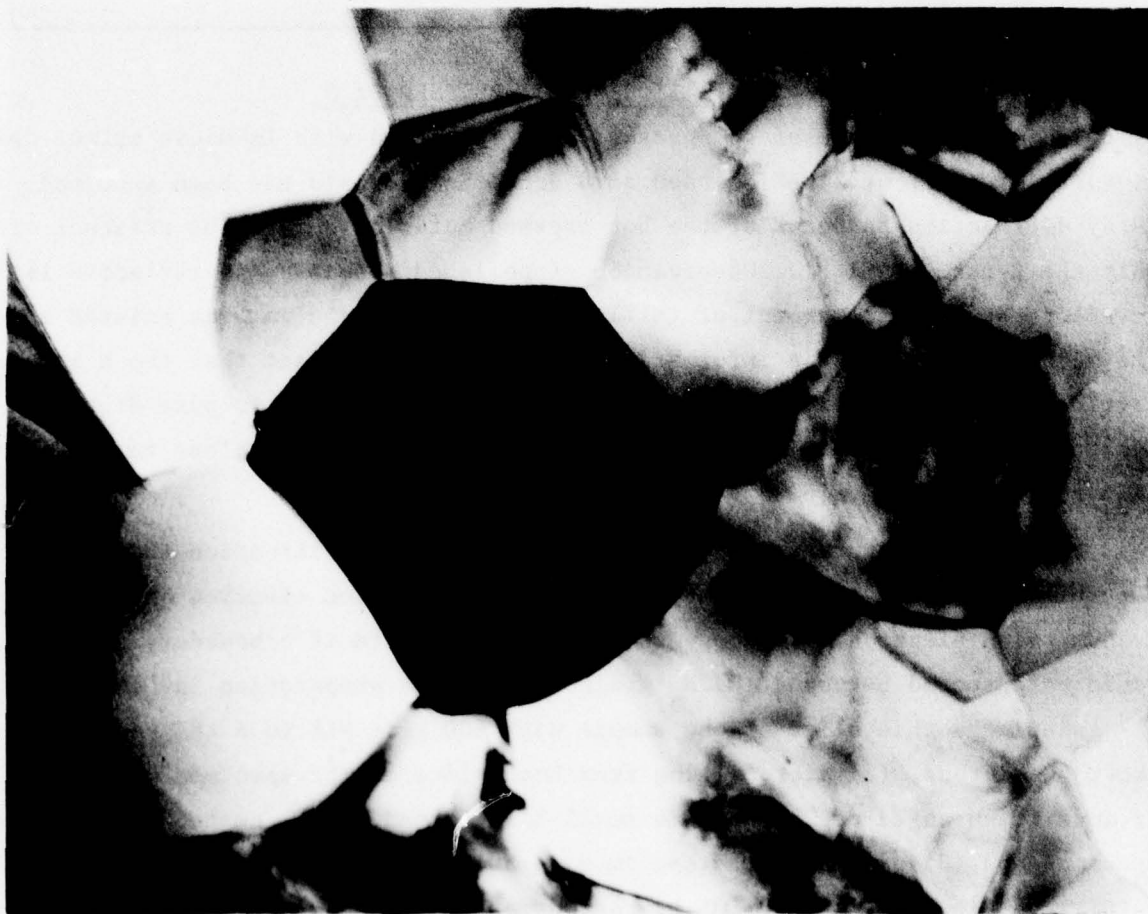


Figure 5. TEM Photomicrograph of the Grain Structure in Hot Pressed Si_3N_4 Containing 7 wt% BeSiN_2 . In-House Si_3N_4 powder used during fabrication. 68,000X.



Figure 6. TEM Photomicrograph of the Grain Structure in Hot Pressed Si_3N_4 Containing 7 wt% BeSiN_2 . In-House Si_3N_4 powder used during fabrication. 150,000X.

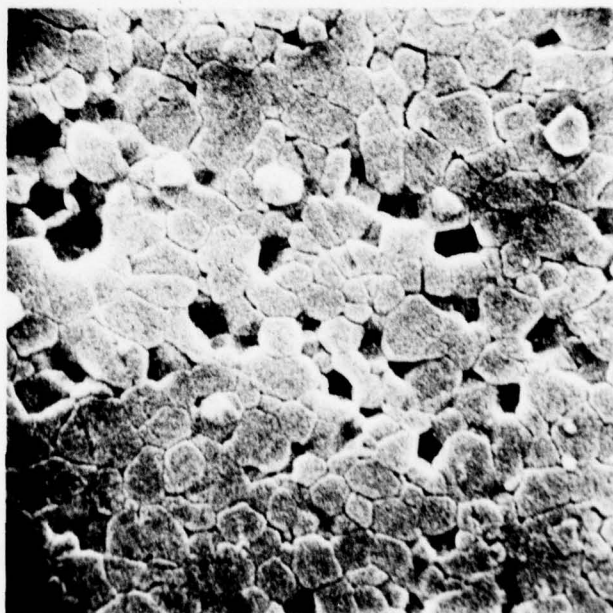


Figure 7. SEM Photomicrograph Showing Grain Size and Morphology of $\beta\text{-Si}_3\text{N}_4$, Hot Pressed Material, 7000X.

Section IV

EVALUATION OF THERMOMECHANICAL PROPERTIES OF HOT PRESSED Si_3N_4 CERAMIC FABRICATED FROM PROCESSED GTE SYLVANIA SN-502 Si_3N_4 POWDER CONTAINING 7% BeSiN_2

A. OXIDATION RESISTANCE

Oxidation of test pieces of hot pressed Si_3N_4 was performed in an Al_2O_3 tube furnace capable of obtaining temperature as high as 1850°C in air. New Al_2O_3 tubes were first baked-out at 1700°C for 24 h to volatilize alkali impurities which may have spurious effects on the oxidation rate of Si_3N_4 . The Si_3N_4 specimen was placed on a SiC setter which lay on an Al_2O_3 boat. This assembly was plunged in two steps into the hot furnace maintained at the desired oxidation temperature. In all cases the oxidation atmosphere was air flowing at $\sim 5\text{cc/sec}$. Specimens were periodically removed from the furnace and their weight measured on a Mettler H54AR balance capable of measuring weight reproducibly to the nearest $2 \times 10^{-5}\text{g}$.

Prior to oxidation the rectangular cross section test bars were cleaned with concentrated HCl and HF separately, and then rinsed in distilled water and dried. The texture of a specimen surface shown in Fig. 8 is typical for all specimens and characteristic of grinding marks with 320 grit diamond used to prepare the thermomechanical test specimens.

The oxidation data gathered for NC-132 and hot-pressed SN-502 Si_3N_4 containing 7% BeSiN_2 is shown in Table VI.

Figures 9 and 10 show plots of the data presented in Table VI in which the square of the weight gain per unit area $(\Delta W/A)^2$ is plotted against oxidation time(t) at the specified temperatures. The data approximate classical parabolic oxidation behavior except for the case of the NC-132 material as shown in Figure 10. This material exhibited substantial oxidation at 1400°C which is nearly parabolic in its behavior up to and exposure time of $\sim 25\text{ h}$, beyond which the materials resistance to oxidation begins to increase and non-linearity sets in. In comparing Figures 9 and 10 it should be emphasized that although in each instance the time coordinate (abscissa) is scaled the same, the ordinate in Figure 10 is scaled 100 times that used in Figure 9. The oxidation behavior for NC-132 as shown in Figure 10 is probably related to time dependent changes in the chemical composition of the oxide scale as can be seen in Figure 9. The most striking result of the oxidation studies is that the use of a small amount of BeSiN_2 as a densification aid gives rise to hot pressed Si_3N_4 with unusually

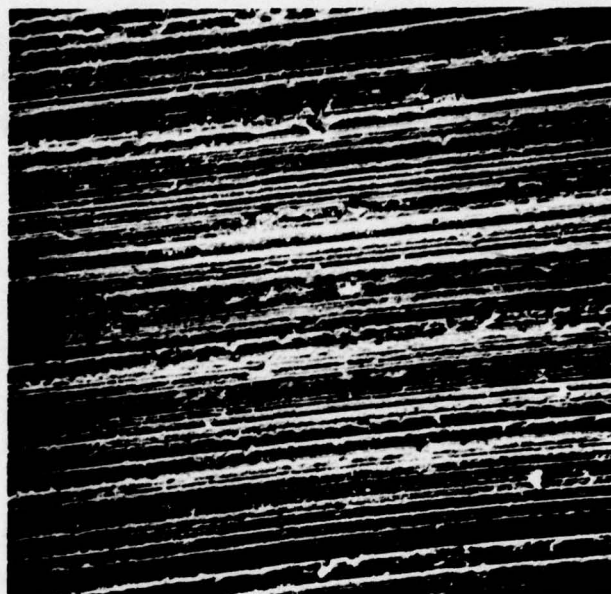


Figure 8. SEM of the Typical Surface Character of Test Bars Used for Oxidation and Mechanical Testing. 200X.

Table VI
WEIGHT GAIN/UNIT AREA VS. TIME IN AIR AT 1405°C FOR NC-132 AND BILLET NO. 3SN(31)
HOT PRESSED FROM PROCESSED SN-502 Si_3N_4 POWDER CONTAINING 7% BeSiN_2

Hot Pressed Billet No. 3Sn-(31)		NC-132	
Time(h)	$\Delta W/A(\text{g/m}^2)$	Time(h)	$\Delta W/A(\text{g/m}^2)$
5.0	0.20	1.5	3.39
17.0	0.28	17.0	7.45
49.0	0.42	26.0	9.00
122.0	0.63	48.0	11.31
209.0	0.74	70.0	13.11
		210.0	17.40

The parabolic rate constant (k) in the expression,

$$\left(\frac{\Delta W}{A}\right)^2 = kt$$

is computed from the 1405°C data plotted in Figure 9 for hot pressed SN-502, Si_3N_4 powder containing 7% BeSiN_2 and a value of $7.4 \times 10^{-13} \text{ Kg}^2/\text{m}^4 \text{ sec.}$ is obtained.

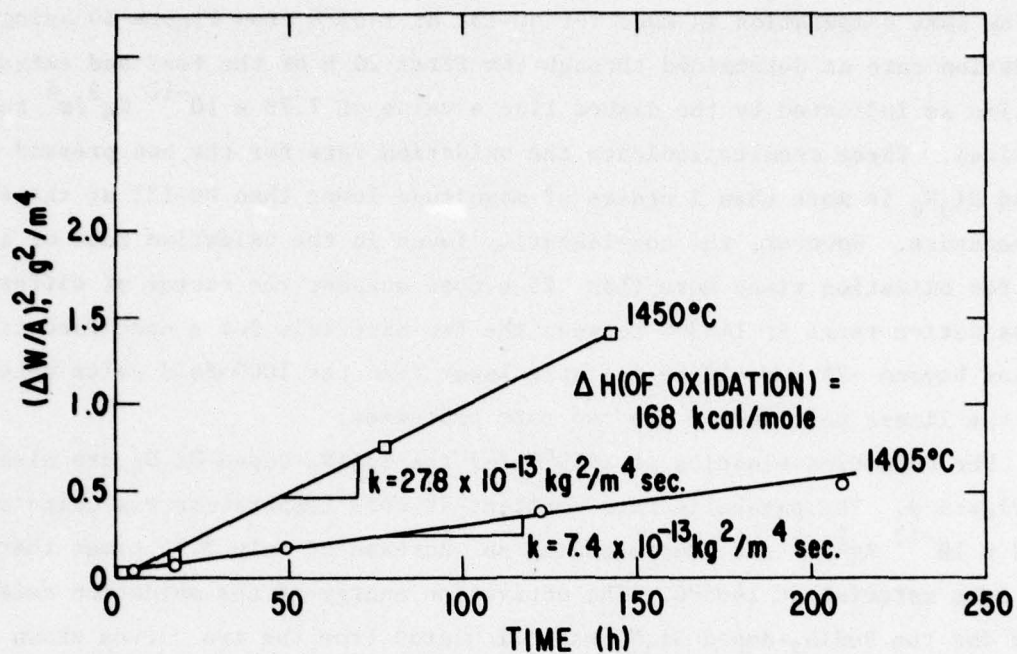


Figure 9. Oxidation Kinetics of Hot Pressed SN-502 Si_3N_4 Powder Containing 7% BeSiN_2

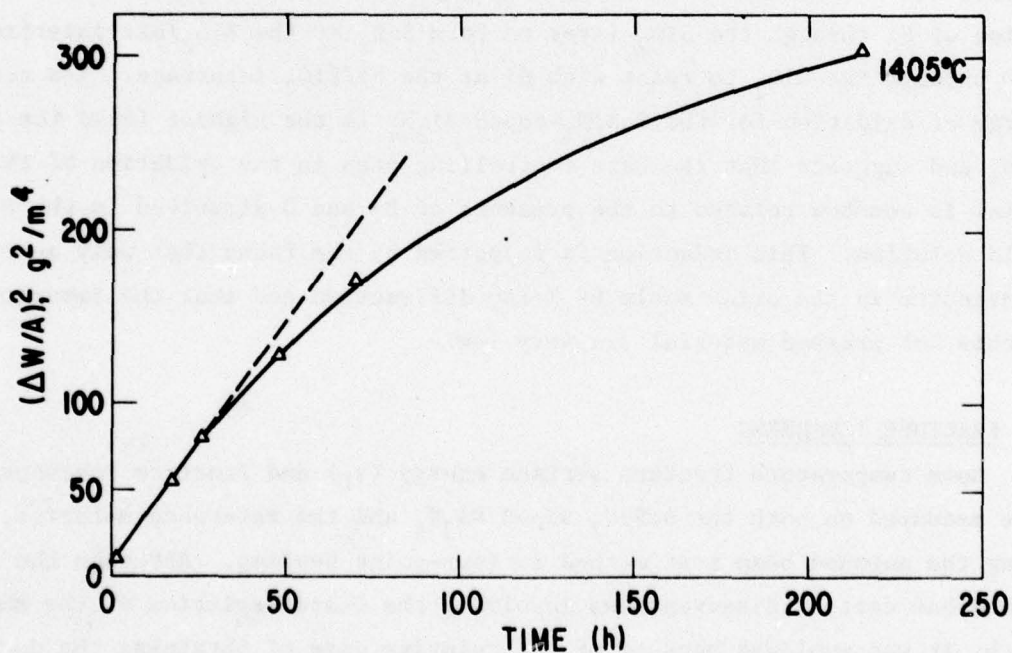


Figure 10. Oxidation Kinetics of Hot-Pressed NC-132 Si_3N_4

If the same computation is made for NC-132 at 1405°C from Figure 10 using the oxidation rate as determined through the first 25 h of the test and extrapolated in time as indicated by the dashed line a value of $7.78 \times 10^{-10} \text{ Kg}^2/\text{m}^4 \text{ sec}$ is obtained. These results indicate the oxidation rate for the hot pressed BeSiN₂ doped Si₃N₄ is more than 3 orders of magnitude lower than NC-132 at the same temperature. However, the non-linearity found in the oxidation rate of the NC-132 for oxidation times more than ~25 h does suggest the factor of difference in oxidation rates at 1405°C between the two materials for a specified time period beyond ~25 h would be a little lower than the 1000-fold value determined for the linear portions of the two rate processes.

The oxidation kinetics at 1450°C for the BeSiN₂ doped Si₃N₄ are also shown in Figure 9. The parabolic rate constant at this temperature was computed to be $27.8 \times 10^{-13} \text{ Kg}^2/\text{m}^4 \text{ sec}$, representing an increase of only 3.75 times that of the same material at 1405°C. The activation energy of the oxidation rate process for the BeSiN₂-doped Si₃N₄ was calculated from the two curves shown in Figure 9. This value was determined to be about 165 Kcal/mole. It is more than twice the value reported⁸ for the oxidation of Si to crystalline SiO₂ in which process the rate controlling process is expected to be either the rate of diffusion of Si through the SiO₂ layer to form SiO₂ at the SiO₂/air interface or of O through the SiO₂ to react with Si at the Si/SiO₂ interface. The activation energy of oxidation for the BeSiN₂-doped Si₃N₄ is the highest found for dense Si₃N₄ and suggests that the rate controlling step in the oxidation of this material is somehow related to the presence of Be and O dissolved in the β-Si₃N₄ solid solution. This deduction is supported by the facts that only α-cristobalite is detected in the oxide scale by X-ray diffraction and that the impurity levels in this hot pressed material are very low.

B. FRACTURE TOUGHNESS

Room temperature fracture surface energy (γ_f) and fracture toughness (K_{IC}) were measured on both the BeSiN₂ doped Si₃N₄ and the reference material, NC-132, using the notched beam test method in four-point bending. Although the test method has certain disadvantages involving the characteristics of the sawed notch, it was employed because of the relative ease of obtaining the desired comparative data between different materials.

Test specimens were cut and sliced out of hot-pressed billets using a 320 grit diamond wheel. The nominal test bar dimensions were 0.38 cm x 0.38 cm x 4.45 cm with the 4 long edges chamfered slightly to smooth out any sharp edge

slicing flaws. A 0.254 mm diamond wheel was used to cut a notch in the center of each test bar to a depth of -1.52 mm resulting in a nominal "crack" depth to test bar thickness or C/D ratio of 0.4. Span dimensions of 3.81 cm and 1.27 cm were used for the outer specimen supports and inner load application points, respectively.

Seven test bars of NC-132 were evaluated for K_{IC} and γ_f using the expressions:

$$K_{IC} = \frac{3PL(\pi C)^{1/2} f(C/D)}{2bD^2}$$

and,

$$\gamma_f = \frac{9P^2 L^2 C}{8 E b^2 D^4} \left[f(C/D) \right]^2,$$

Where:

P = Load to Fracture

L = Span

C = Crack Depth

b = Specimen Width

D = Specimen Depth

f = (C/D) = Geometric Function According to TADA⁹ et al

$$= 1.122 - 1.4(C/D) + 7.33(C/D)^2 - 13.08(C/D)^3 + 14.0(C/D)^4$$

E = Young's Modulus.

Table VII shows the individual values of K_{IC} and γ_f for NC-132 at room temperature obtained for the seven test specimens evaluated.

TABLE VII	
ROOM TEMPERATURE K_{IC} and γ_f FOR NC-132 Si_3N_4	
K_{IC} (MN m ^{-3/2})	γ_f (ergs cm ⁻²)
6.32	20,445
6.82	23,658
7.31	27,865
7.39	28,265
8.21	34,408
7.35	27,589
<u>7.41</u>	<u>28,242</u>
Average: 7.26	27,210

The test specimens for evaluating the K_{IC} and γ_f for the BeSiN_2 -doped SN-502 Si_3N_4 were cut from a single billet to nominal dimensions of 0.355 cm x 0.355 cm x 4.06 cm. These test bars were notched to a depth of ~1.39 mm to give a nominal C/D ratio of ~.4. In this instance 8 test bars were evaluated using the same expressions for K_{IC} and γ_f as above. The results of these determinations are shown in Table VIII.

TABLE VIII	
ROOM TEMPERATURE K_{IC} and γ_f FOR PROCESSED SN-502 Si_3N_4 POWDER CONTAINING 7% BeSiN_2	
$K_{IC} (\text{MNm}^{-3/2})$	$\gamma_f (\text{ergs cm}^{-2})$
4.52	10,539
3.81	7,488
4.04	8,400
4.18	9,028
4.01	8,314
4.49	10,432
3.92	7,910
<u>3.54</u>	<u>6,462</u>
Average: 4.06	8,571

Comparing the room temperature values of K_{IC} and γ_f of the two materials it is apparent that these properties are clearly superior in the NC-132 material. During the fabrication of the BeSiN_2 doped Si_3N_4 specimens it was discovered that much more care had to be taken in grinding these bars than was required for the NC-132 test specimens. In fact, to avoid chipping, a 500 grit diamond wheel had to be used whereas a 320 grit wheel was satisfactory for the NC-132. That experience encountered before actually running the test bars indicated that the single-phase material exhibited a lower fracture toughness as compared with the NC-132 polyphase material.

The values for K_{IC} and γ_f for the BeSiN_2 -doped Si_3N_4 approximate quite closely to those of ~3.8 $\text{MN m}^{-3/2}$ and 10,000 ergs cm^{-2} determined in this laboratory for sintered SiC.

C. CREEP RESISTANCE

Creep strain rates were determined for both the BeSiN_2 doped Si_3N_4 and the reference material NC-132. Test bars were loaded in a three-point bending mode using SiC fixtures. The configuration of test specimen and support and loading fixtures are shown in Figure 11. These parts all operated in a 15 cm x 15 cm x 15 cm box furnace equipped with 6" Super Kanthal 33" heating elements. The furnace was capable of operating in air at 1600°C.

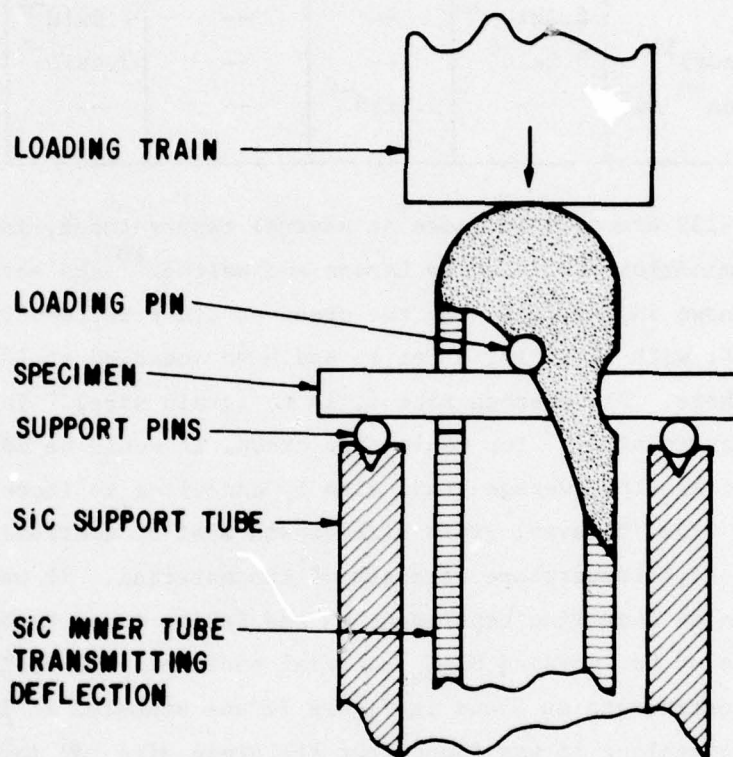


Figure 11. Configuration of Creep Test Specimen, Supports and Loading Fixtures

Deflection of the test specimen was measured with a DC-operated LVDT (Linear Variable Differential Transformer) manufactured by Schaevitz Engineering Model Number 050 DC-D. This model LVDT operated with a sensitivity of ~ 80 V/cm.

Test specimens of both Si_3N_4 materials to be evaluated were nominally 2.54 mm x 2.54 mm x 2.80 cm long. When assembled and under test, the specimen was stressed by dead weight loading external to the furnace. The span of the specimen under load was 2.235 cm.

Strain rates were measured as a function of both temperature and stress. Table IX shows the result of creep measurements at a stress of 69 MN m^{-2} at temperatures up to 1500°C (where the material allowed it). Some literature

TABLE IX
STRAIN RATE MEASUREMENTS ($\dot{\epsilon}$, h⁻¹) AS A FUNCTION OF TEMPERATURE

$\sigma = 69 \text{ MN m}^{-2}$	1250°C	1300°C	1350°C	1400°C	1450°C	1500°C
GE, HPSN with 7% BeSiN ₂	--	--	1.82x10 ⁻⁶	8.4x10 ⁻⁶	4.6x10 ⁻⁵	--
GE, HPSN with 7% BeSiN ₂ (Annealed)	--	--	--	2.5x10 ⁻⁶	2.1x10 ⁻⁵	5.6x10 ⁻⁵
NC-132	6.2x10 ⁻⁵	--	--	7.8x10 ⁻⁴	--	--
NC-132 (Seltzer) ¹¹	3.0x10 ⁶	--	--	3.4x10 ⁻⁴	--	--
NC-132 (Larsen ¹⁰ and Walther)	--	3.2x10 ⁻⁴	--	--	--	--

data for NC-132 are also included at several temperatures, including a single-point determination published by Larsen and Walther¹⁰ and several by Seltzer¹¹.

Also shown in the table are the creep strain rate results of the GE hot-pressed Si₃N₄ with 7% BeSiN₂ after it had been annealed at 1725°C for 24 h in a N₂ atmosphere. Since creep rate $\dot{\epsilon}$ is to (grain size)⁻² for Nabarro-Herring creep and (grain size)⁻³ for Coble-type creep, it would be advantageous to be able to increase the average grain size by annealing to improve creep resistance. At the same time, however, grain size growth must be controlled so as not to degrade the high temperature strength of the material. It was therefore decided to run an annealing experiment on the BeSiN₂ doped Si₃N₄.

A piece of hot pressed Si₃N₄ material containing 7% BeSiN₂ having a preannealed microstructure as shown in Figure 12 was annealed at 1725°C for 25 h in N₂. After annealing it was found that the grain size had indeed increased from an average of ~0.5 μ to ~1.1 μ . The microstructure of the annealed specimen was that shown in Figure 13.

A creep test bar was annealed under the same conditions as described and evaluated for its creep resistance as a function of temperature at 1400°C, 1450°C and 1500°C, with the results shown in Table IX.

When the data shown in Table IX are plotted in the form of log $\dot{\epsilon}$ vs. $\frac{1}{T}$ they appear as shown in Figure 14. These data indicated that at 1400°C and 69 MN/m² the BeSiN₂ doped Si₃N₄ material had a creep resistance more than an order of magnitude greater than the reference material.

It is also noted from Figure 14 that the GE hot-pressed Si₃N₄ with 7% BeSiN₂ after the annealing treatment did improve in creep resistance by just about a factor of 3. The increase in average grain size by a factor of ~2.2 due to the



Figure 12. Microstructure of As-Hot Pressed SN-502 Si_3N_4 Powder Containing 7% BeSiN_2 - 9,765X.

annealing process would, according to pure Nabarro-Herring type of creep, result in about a 5 times improvement in creep resistance as compared to an 11 times improvement if the creep mechanism was pure Coble type. Considering inaccuracies in the estimates of grain sizes it would appear that Nabarro-Herring or bulk diffusion is the predominate creep mechanism in the BeSiN_2 doped Si_3N_4 material.

The activation energy of creep was determined for the BeSiN_2 doped Si_3N_4 and NC-132 from the data presented in Figure 14. These determinations indicated ΔH values for the BeSiN_2 doped materials to be $\sim 180 \text{ Kcal mole}^{-1}$ for both the annealed and unannealed forms. The ΔH for NC-132 was computed to be $130 \text{ Kcal mole}^{-1}$.

The dependence of creep on stress was also studied for both NC-132 and the BeSiN_2 doped material. The results of these studies are shown in Table X and plotted as shown in Figure 15. Data from the literature for NC-132 are also included for additional comparison purposes.



Figure 13. Microstructure of Hot-Pressed Sn-502 Si_3N_4 Powder Containing 7% BeSiN_2 After Annealing in N_2 at 1725°C for 25 h - 7,875X.

The data obtained for the BeSiN_2 doped Si_3N_4 indicate a power law stress dependence with a stress exponent $n = 1.1$ which appears to corroborate the findings in the grain growth experiment, that the creep mechanism in this material is primarily of the Nabarro-Herring or bulk diffusion type.

D. STRENGTH

Modulus of rupture determinations were conducted on NC-132 and on the hot pressed, processed SN-502 Si_3N_4 powder containing 7% BeSiN_2 . Tests, including time to failure determinations, were made at temperatures up to 1400°C .

The test bars were nominally 0.38 cm x 0.38 cm x 4.44 cm long, surface finished and chamfered on the 4 long edges with 320 grit diamond wheel. As reported in a previous section the BeSiN_2 doped material had to be finish-ground with a 500 grit diamond wheel to avoid excessive edge chipping.

Tests were conducted in a three-point bending mode with a 3.81 cm span between supports.

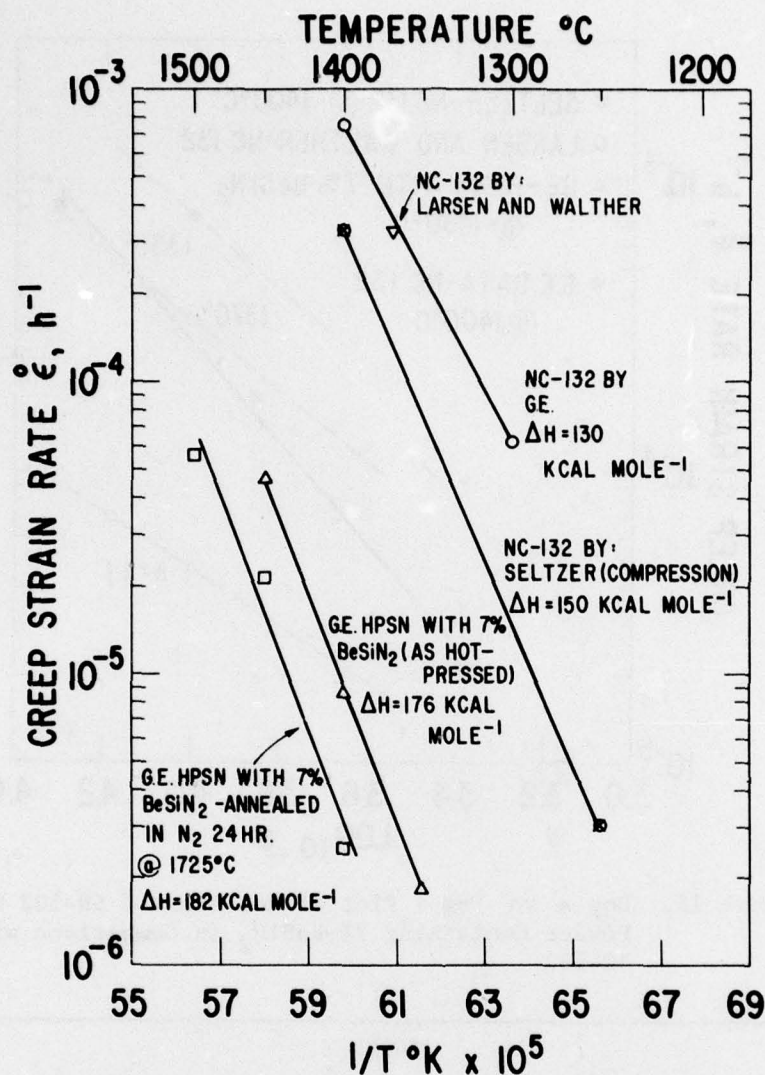


Figure 14. Log $\dot{\epsilon}$ vs $1/T^{\circ}\text{K}$ Plot of Annealed and Unannealed Hot Pressed SN-502 Si_3N_4 Powder Containing 7% BeSiN_2 in Comparison with NC-132

A comparison of short time strengths between NC-132 and the BeSiN_2 doped Si_3N_4 at room temperature and at 1400°C is shown in Table XI and in Figure 16. Although the BeSiN_2 doped material displayed considerably lower strengths than NC-132 when measured at room temperature, its 1400°C fracture strength indicated it retains 88% of its room temperature strength at temperature. The NC-132 material at 1400°C was found to have lost ~65% of its room temperature strength. This comparison is shown graphically on the bar chart to the right of Figure 16.

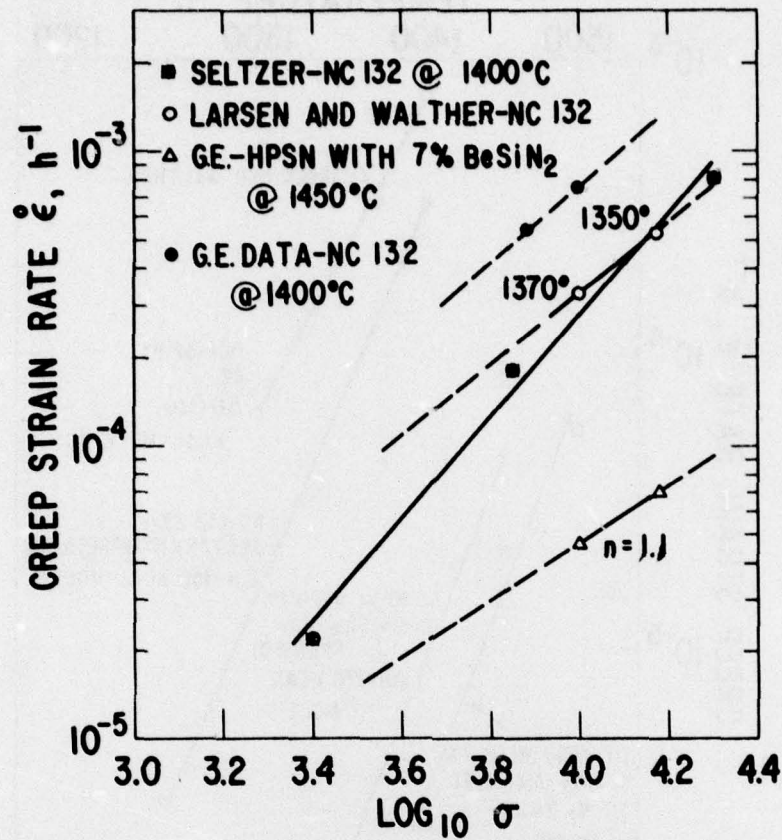


Figure 15. Log $\dot{\epsilon}$ vs Log σ Plot of Hot Pressed SN-502 Si_3N_4 Powder Containing 7% BeSiN_2 in Comparison with NC-132

TABLE X STRAIN RATE MEASUREMENTS ($\dot{\epsilon}, \text{h}^{-1}$) AS A FUNCTION OF STRESS					
Stress (MN/m^2)	17	48	69	103	138
GE Hot Pressed Si_3N_4 Containing 7% BeSiN_2 (1450°C)	--	--	4.6×10^{-5}	6.8×10^{-5}	--
NC-132 (1400°C)	--	5.3×10^{-4}	7.8×10^{-4}	--	--
NC-132 (Seltzer) (1400°C)	2.2×10^{-5}	1.8×10^{-4}	--	--	8.0×10^{-4}
NC-132 (Larsen and Walther) (1350°C)	--	--	3.2×10^{-4}	5.1×10^{-4}	--

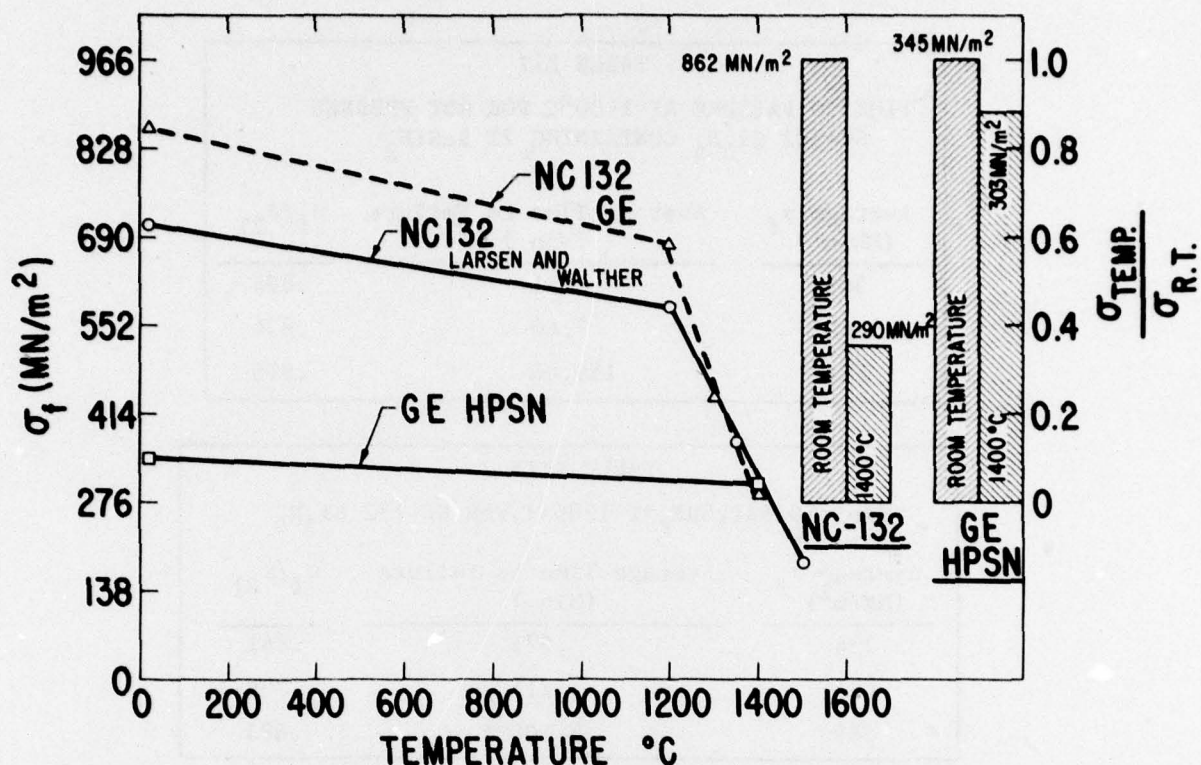


Figure 16. Stress vs. Temperature for Hot Pressed SN-502 Si_3N_4 Powder Containing 7% BeSiN_2 in Comparison with NC-132

TABLE XI		
SHORT TIME MODULUS OF RUPTURE AT ROOM TEMPERATURE AND AT 1400°C		
	σ_{RT}	$\sigma_{1400^\circ\text{C}}$
NC-132 (GE) (3 PT-Bend)	862 MN/m ²	290 MN/m ²
NC-132 (IITRI) (4 PT-Bend)	710	370 (1350°C) 183 (1500°C)
GE, HPSN (3 PT-Bend)	345	303

Time to failure determinations were made on the hot-pressed Si_3N_4 with BeSiN_2 at 1400°C and compared with another set of time to failure tests on NC-132 conducted at 1200°C.

Three different crosshead speeds were employed to obtain three different stressing rates for each material. The results of these tests are shown in Tables XII and XIII for the BeSiN_2 doped material and NC-132, respectively. When these data are plotted with σ_f/σ_{RT} vs time to failure the results are shown in Figure 17. If the resulting plots are extrapolated out to 10,000 h,

TABLE XII		
TIME TO FAILURE AT 1400°C FOR HOT PRESSED SN-502 Si_3N_4 CONTAINING 7% BeSiN_2		
Average σ_f (MN/m ²)	Average Time to Failure (Min.)	σ_f/σ_{RT}
305	0.71	.884
288	7.40	.834
281	159.00	.816

TABLE XIII		
TIME TO FAILURE AT 1200°C FOR NC-132 Si_3N_4		
Average σ_f (MN/m ²)	Average Time to Failure (Min.)	σ_f/σ_{RT}
724	.071	.841
678	.715	.786
589	8.100	.683

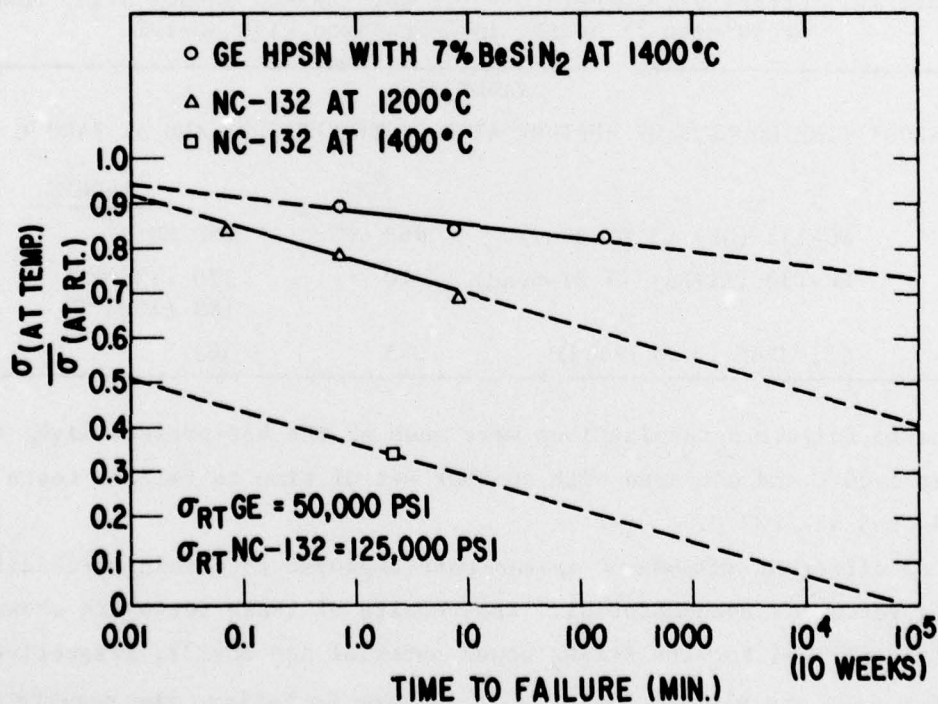


Figure 17. Time to Failure vs Relative Strength at Temperature

they indicate a strength of 240 MN/m^2 at 1400°C for the BeSiN_2 doped material and 269 MN/m^2 for the NC-132 material at 1200°C .

A single point was obtained for the NC-132 at 1400°C which is shown in Figure 17 as an open square. If it is assumed that the time to failure curve through that one point were to follow the same slope as the NC-132 curve at 1200°C (a conservative assumption), it would have zero strength after 1600 h at 1400°C .

Section V

CONCLUSIONS

Although the studies in this investigation were made on a Si_3N_4 powder composition unoptimized with regard to powder processing, the overall results of the investigation indicate that Si_3N_4 ceramic containing small additions of BeSiN_2 has a high potential for becoming the only Si_3N_4 ceramic useful at temperatures up to 1400°C .

If the room temperature modulus of rupture value of 345 MN/m^2 and the K_{IC} value of $4.0 \text{ MN m}^{-3/2}$ determined in this work are used to compute the critical flaw size in this material, from the expression:

$$K_{\text{IC}} = \sigma_f (\pi C)^{1/2} f(C/D)$$

one obtains a C value of 35.3μ .

It seems certain that with careful processing of the powder that a maximum flaw size of 10μ could be achieved, which in turn would indicate a room temperature modulus of rupture of more than 650 MN/m^2 should result.

Additionally, if the 650 MN/m^2 room temperature material retained 88% of that value at 1400°C as has been indicated by this work, it seems quite probable that a 575 MN/m^2 ($>80,000 \text{ psi}$) at 1400°C Si_3N_4 ceramic is an achievable goal.

Progress has been made in other studies in this laboratory showing that Si_3N_4 powders processed in the same way as described in this report with small additives of BeSiN_2 can be die pressed and sintered to densities ~98% of theoretical. Although extensive evaluation of the thermomechanical properties of the sintered material has not been made, the results obtained to date indicate that the superior properties observed in this investigation of the hot-pressed form of Si_3N_4 will be achieved in the sintered ceramic.

This investigation has shown the current composition, $(\text{Si}_{2.9}\text{Be}_{0.1}\text{N}_{3.8}\text{O}_{0.2})$, of the hot-pressed BeSiN_2 -doped Si_3N_4 to have γ_f and K_{IC} values at room temperature which approximate those of SiC . It was determined in a single experiment that if 5% sub-micron SiC powder was mixed in with the BeSiN_2 -doped Si_3N_4 powder a 14% increase in fracture toughness was noted in the resulting hot pressed ceramic. It would appear that this experiment offers some considerable hope that the fracture toughness and surface fracture energy of this new form of Si_3N_4 can be materially improved and probably without any degradation of its otherwise superior thermomechanical properties.

REFERENCES

1. C.D. Greskovich, J.H. Rosolowski, S. Prochazka: "Ceramic Sintering" Final Report on Contract No. N00014-74-C-0331, Aug., 1975, S.R.D.-75-084.
2. B.J. Wuench, T. Vasilos: "Self-Diffusion in Silicon Nitride" Final Report Contract No. N00014-73-C-0212, March, 1975.
3. K. Kijima and S. Shirasaki, "Nitrogen Self-Diffusion in Si_3N_4 ," J. Chem. Phys., 65(7) 2668-71(1976).
4. R.J. Charles: "Diffusion Controlled Stress Rupture of Polycrystalline Materials." Submitted to Metal Trans. A, Vol. 7A, HP 1081-89(1976).
5. C.D. Greskovich, S. Prochazka, and J.H. Rosolowski, "Basic Research on Technology Development for Sintered Ceramics," Report No. AFML-TR-76-179, November, 1976.
6. K.S. Mazdiasni and C.M. Cooke, "Synthesis Characterization and Consolidation of Si_3N_4 Obtained from Ammonolysis of SiCl_4 ," J. Amer. Ceram. Soc., 56 628(1973).
7. I.C. Huseby, H.L. Lukas, and G. Petzow, "Phase Equilibria in the System Si_3N_4 - SiO_2 - BeO - Be_3N_2 ," J. Amer. Ceram. Soc., 58(9-10) 377-380(1975).
8. W.C. Tripp, J.W. Hinze, M.G. Mendiratta, R.H. Duff, A.F. Hampton, J.E. Stroud and E.T. Rodine, "Internal Structure and Physical Properties of Ceramics at High Temperatures," Final Report No. ARL-TR-75-0130, June, 1975.
9. H. Tada, P. Paris and G. Irwin, "The Stress Analysis of Cracks Handbook," Del Research Corp., Hellertown, Pennsylvania(1973).
10. D.C. Larsen and G.C. Walther, "Property Screening and Evaluation of Ceramic Vane Materials," Air Force Materials Laboratory, Report No. IITRI-D6114-ITR-24, Oct. 1977, IIT Research Institute, Chicago, Illinois 60616.
11. Martin S. Seltzer, "High Temperature Creep of Silicon-Base Compounds," Bulletin Amer. Ceram. Soc. Vol. 56 No. 4(1977) 418-423.

PRECEDING PAGE BLANK

DISTRIBUTION LIST

(One copy unless otherwise noted)

(3 copies plus balance after distribution)

U.S. Naval Air Systems Command

(AIR-52031B)

Department of the Navy

Washington, DC 20361

(7 copies, for internal distribution by AIR-954, as follows)

AIR-954 (2 copies); AIR-536B1 (1 copy); AIR-330A (1 copy);

AIR-330B (1 copy); AIR-5361A (1 copy); AIR-5362A (1 copy)

U.S. Naval Air Systems Command

(AIR-954 - 7 copies)

Department of the Navy

Washington, DC 20361

(2 copies)

Commander, Naval Air Development Center

Code 302A, A. Fletcher (1 copy)

Code 30232, E. Tankins (1 copy)

Warminster, PA 18974

U.S. Naval Air Propulsion Test Center (2 copies)

Attn: J. Glatz (PE-43 - 1 copy)

A. Martino (AT-1 - 1 copy)

1440 Parkway Ave.

Trenton, NJ 08628

U.S. Naval Sea Systems Command

Code 0352

Department of the Navy

Washington, DC 20362

Commander, Naval Weapons Center

Code 5516

China Lake, CA 93555

U.S. Naval Ships Engineering Center

Code 6146 - Department of the Navy

National Center, Building 4

Washington, DC 20362

Naval Weapons Laboratory

Attn: W. Mannschreck

Dahlgren, VA 22448

U.S. Naval Ships Research and Development Center

Code 2812

Annapolis, MD 21402

PRECEDING PAGE BLANK

DISTRIBUTION LIST (Cont'd)

Naval Surface Weapons Center
Metallurgy Division
White Oak
Silver Spring, MD 20910

(2 copies)

Director
Naval Research Laboratory
Code 6360 (1 copy)
Code 6400 (1 copy)
Washington, DC 20375

Office of Naval Research
The Metallurgy Program, Code 471
Arlington, VA 22217

Director
Army Materials and Mechanics Research Center
(A. Gorum)
Watertown, MA 02172

Commanding Officer
Army Research Office Durham
Box CM, Duke Station
Durham, NC 27706

U.S. Army Aviation Materials Laboratories
Fort Eustis, VA 23604

Air Force Materials Laboratory
Code LLM
Wright-Patterson Air Force Base
Dayton, OH 45433

Air Force Office of Scientific Research
ATTN: Major W.C. Simmons
1400 Wilson Boulevard
Arlington, VA 22209

Air Force Propulsion Laboratory
Code TBP
Wright-Patterson Air Force Base
Dayton, OH 45433

National Aeronautics and Space Administration
Code RWM
800 Independence Ave., SW
Washington, DC 20546

DISTRIBUTION LIST (Cont'd)

(3 copies)

National Aeronautics and Space Administration
Lewis Research Center
C.M. Ault (1 copy)
H.P. Probst (1 copy)
W.A. Sanders, MS-49-1 (1 copy)
21000 Brookpark Road
Cleveland, OH 44135

U.S. Department of Energy
Division of Reactor Development
Mail Station F-309 (A. Van Echo)
Washington, DC 20545

U.S. Department of Energy
Materials and Fabrication Technology Branch
Office of Conservation
20 Massachusetts Ave., NW
Washington, DC 20545

Metals and Ceramics Information Center
Battelle Columbus Laboratories
505 King Ave.
Columbus, OH 43201

The John Hopkins University
Applied Physics Laboratory
(Maynard L. Hill)
Johns Hopkins Road
Laurel, MD 20810

AVCO RAD
201 Lowell Street
Wilmington, MA 01887

ITT Research Institute
10 West 35th St.
Chicago, IL 60610

Detroit Diesel Allison Division
General Motors Corporation
Materials Laboratories
Indianapolis, IN 46206

Pratt and Whitney Aircraft Division
United Aircraft Co.
East Hartford, CT 06108

United Technologies Research Center
United Aircraft Co.
East Hartford, CT 06108

DISTRIBUTION LIST (Cont'd)

Pratt and Whitney Aircraft
(Mr. A. Magid)
Florida Research and Development Center
West Palm Beach, FL 33402

Westinghouse Electric Company
Materials and Processing Laboratory
(Ray Bratton)
Beulah Road
Pittsburgh, PA 15235

Westinghouse Electric Company
Lester Branch 9175
Philadelphia, PA 19113

Chief, Materials Engineering Dept.
Dept. 93-39M
Air Research Manufacturing Co. of Arizona
402 South 36th Street
Phoenix, AZ 85034

Lycoming Division
AVCO Corporation
Stratford, CT 06497

Curtis Wright Company
Wright Aeronautical Division
Wood-Ridge, NJ 07075

Bell Aerosystems Company
Technical Library
P.O. Box 1
Buffalo, NY 14240

General Electric Company
Aircraft Engine Group
Materials and Processes Technology Laboratories
Evendale, OH 45215

Solar
(Dr. A. Metcalfe)
2200 Pacific Highway
San Diego, CA 92112

Teledyne CAE
1330 Laskey Road
Toledo, OH 43601

DISTRIBUTION LIST (Cont'd)

Stellite Division
Cabot Company
Technical Library
P.O. Box 746
Kokomo, IN 46901

Norton Company
Protective Products Division
(N.J. Ault)
Worcester, MA 01606

Research Library and Development Division
The Carborundum Company
P.O. Box 337
Niagara Falls, NY 14302

Ford Motor Company
Product Development Group
(E.A. Fisher)
2000 Rotunda Drive
Dearborn, MI 48121

General Electric Company
AEG Technical Information Center
Mail Drop N-32, Bldg. 700
Cincinnati, OH 45215

Professor Richard E. Tressler
Ceramic Science Section
Pennsylvania State University
201 Mineral Industries Bldg.
University Park, PA 16802

Dr. T.D. Chikalla
Ceramics and Graphite Section
Battelle-Northwest Laboratories
Richland, WA 99352

TRW Equipment Laboratories
23555 Euclid Ave.
Cleveland, OH 44117

Deposits and Composites, Inc.
ATTN: R.E. Engdahl
318 Victory Drive
Herndon, VA 22070

FINAL REPORT ONLY (12 COPIES FOR DDC)
Naval Air Systems Command
ATTN: AIR-954 (For DDC)
Department of the Navy
Washington, DC 20361

AD-A057 338

GENERAL ELECTRIC CORPORATE RESEARCH AND DEVELOPMENT --ETC F/G 11/2
SILICON NITRIDE FOR AIRBORNE TURBINE APPLICATIONS.(U)
JUL 78 J A PALM, C D GRESKOVICH

N00019-77-C-0259

UNCLASSIFIED

SRD-78-076

NL

2 OF 2

AD
AO 57338

SUPPLEMENTARY

INFORMATION

END
DATE
FILMED

12-78

DDC

SUPPLEMENTARY

INFORMATION

AD-A057338

ERRATA

FOR

SILICON NITRIDE FOR AIRBORNE TURBINE APPLICATIONS

John A. Palm

Charles D. Greskovich

General Electric Company
Corporate Research and Development
Schenectady, NY 12301

(Prepared under Contract N00019-77-C-0259)

SRD-78-076

p. 26 Add directly under Table VI the following,
high oxidation resistance. If

p. 26 Last line - Delete and

p. 29 The expression $\gamma_f = \frac{9P_L^2 C}{8 E b^2 D^4} \left[f(C/D) \right]^2$ should read

$$\gamma_f = \frac{9P_L^2 C \pi}{8 E b^2 D^4} \left[f(C/D) \right]^2 \quad \text{and;}$$

values for $\gamma_f(\text{ergs cm}^{-2})$ in Table VII should be higher by
a factor of π times.

p. 30 Values for $\gamma_f(\text{ergs cm}^{-2})$ in Table VIII should be higher
by a factor of π times.